II International Congress of Biomathematics

Buenos Aires, Argentina September 14, 1984

Constant field electrode theory and chronic pacing of the heart [1]

Roberto Suárez Ántola

Former Professor of Applied Mathematics
Institute of Exact Sciences
School of Humanities and Sciences
University of the Republic, Montevideo, Uruguay

Abstract A brief physical-mathematical analysis of the electric stimulation of myocardium by current pulses delivered by pacing electrodes is done, introducing two hypothetical continua, electrically coupled, and partially superposed in space. From this analysis some desirable properties of the electric current field produced by the active electrodes are established. A theorem due to Prim is used as a guide to select possible shapes to be given to the active electrode heads to produce electric current fields with the established geometric properties.

Key words: Artificial cardiac pacing, electrode design, concave electrodes, classical field theory, Prim's Theorem, excess mean curvature, critical regions, cardiac stimulation thresholds, physiological threshold increment, limit threshold charges, ventricular liminal regions, electrode polarization, mechanical and electrical hysteresis.

(A) Introduction

In the framework of artificial cardiac pacing, when the target region is close enough to the surface of the pacing electrode, there is evidence about a strong influence of the shape and size of electrode's head on both, acute and chronic pacing threshold, and on the sensing performance of the electrode, ((G) 11, (G) 12, (G) 13, (G) 16, G (19)).

[1] **English translation of the 1984 paper "Teoría del electrodo de campo constante para la cardioestimulación eléctrica crónica" with additional bibliography and comments. The original bibliography is cited as (G) followed by the corresponding reference number. The additional bibliography is cited as (H) followed by the corresponding reference number. Comments are given as footnotes.**

The influence of the size and shape of the head of the electrode seems to be due mainly to the geometry of the electric current field generated by the electrode in the volume conductor

formed by the biological tissues, and to the position of the target region (when pacing) or of the signal source (when sensing) in this volume conductor.
All the procedures that aim to the electric stimulation of the heart can be understood using the following electrophysiological principle ((G) 7, (G) 8, (G) 14, G (16)):

For a successful stimulation a critical quantity of electric charge must be transported through the excitable membranes of a suitable region (Lindeman's **liminal region**) of myocardium depolarizing these membranes over a threshold membrane voltage, so that an action potential can emerge and propagate.

To produce the above-mentioned charge transference, a transient electric current field (pulse) is produced by an active electrode located adjacent to the heart tissue that must be stimulated. To pace the heart a suitably spaced sequence of pulses must be applied.
Now, let us consider the head of an intra-cavity electrode touching the right ventricular endocardium, at the end of a pacemaker lead, as shown in Figure 1.

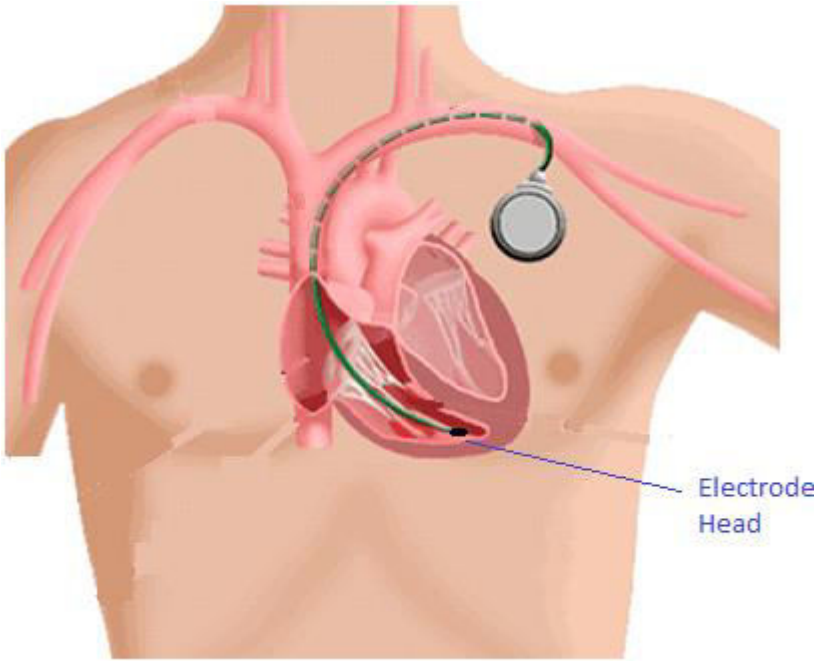

Figure 1: An active electrode is located at the tip of a catheter that is introduced (following a venous path) in the right cardiac cavity.

Once the electrode is implanted, the presence of the foreign materials produces an inflammatory reaction followed by the formation of a capsule of fibrous tissue that surrounds the electrode's head. The local properties of the volume conductor change.

As consequence, the so-called physiological increment of the stimulation threshold is produced ((G) 5, (G) 16, G (19)). Sometimes this ends chronic pacing due to an exit block: the pulse amplitude is too small to overcome the increased threshold. The capsule is sketched in the following Figure 2.

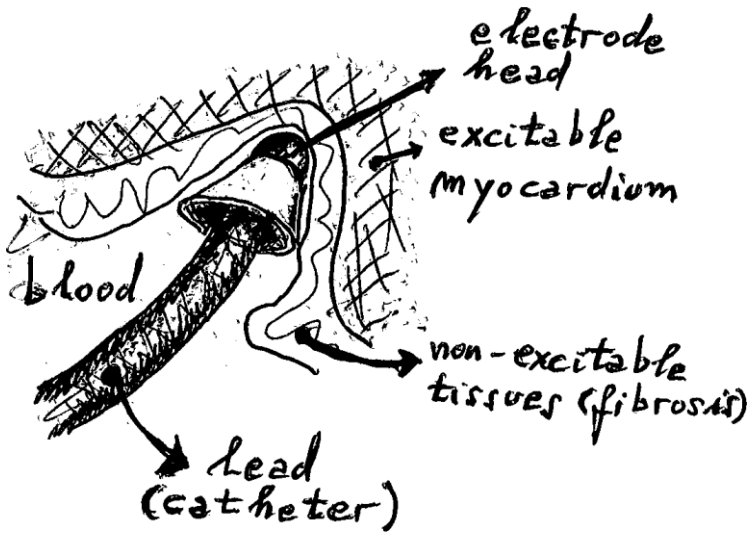

Figure 2: A sketch of the electrode lead with the electrode head separated from the excitable myocardium by fibrotic tissues.

Besides, the relative movement between the electrode and the tissues, due to the contraction of the heart muscle, modifies the distance between the surface of the electrode head and the excitable myocardium. This distance variation is greater the stiffer is the catheter, and could produce an effect of mechanical hysteresis on the pacing thresholds. This mechanical effect could combine with an electric hysteresis effect (called Wedensky effect, see (G) 3).
In the interface between the material of the active electrode head and the tissues, an electrochemical double layer appears. It is modified when an electric current pulse is applied by the artificial pacemaker. If the pacemaker produces a pulse of controlled voltage, the progressive polarization of the double layer during the pulse increases the impedance at the interface. As consequence the amplitude of the stimulating electric current pulse decreases.

So, a system with strongly interacting subsystems is formed by the electrode and the tissues, whose electric, electrochemical, mechanical and biological properties must be taken into account in pacemaker electrode design. From a point of view that stresses a functional description of the signal flow through the system (like the one proposed in G (21)), it is convenient to distinguish four subsystems, partially superposed in space: [2]

[2] **A more detailed description and discussion of these subsystems is given in H (8).**

(a) A passive electric subsystem formed by four moduli connected in series: the electrode lead and head of the active electrode, the interface with biological tissues, the capsule of fibrous tissue that surrounds the electrode's head, and the rest of the tissues ending in the indifferent electrode. Here the input is a current pulse that goes through each module between the electrodes.

(b) An active electric subsystem formed by three moduli connected in series: the target myocardium near the active electrode, the rest of the excitable membranes of the cardiac muscle and the natural pacemaker. An electric signal output from the passive electric subsystem constitutes the input to the active electric subsystem. There are two outputs: an ECG signal and a physicochemical signal.

(c) An active mechanical subsystem formed by the cardiac muscle receives the physicochemical signal from the active electric subsystem and contracts, producing a kinetic output.

(d) A passive mechanical subsystem surrounding the active electrode's head receives as input the above mentioned kinetic output from the active mechanical subsystem, and produces a kinematic output. This signal inputs in the passive electric subsystem, modifying the thickness of the capsule of fibrous tissue that surrounds the electrode's head and varying the distance between the active electrode and the target myocardium.

To simplify the mathematical modelling of this electrode-myocardium system, two facts must be considered:

(1) There is a difference in order of magnitude in the electric resistance between of cell membranes from one side and of extracellular and intracellular compartments from the other side.

(2) It is possible to distinguish four widely separated time scales in artificial cardiac pacing:
(a) A scale of microseconds associated with the transients in tissues electrolytes reordering and inductive phenomena in the electrode lead.
(b) A scale of milliseconds associated with the duration of pacing pulses and with the transport and capacitive phenomena that appear at the interface between the electrode and the biological tissues (electrochemical double layer).
(c) A scale of tenths of seconds, that corresponds to the phases of cardiac cycle and to the mechanical phenomena in the electrode-myocardium system.
(d) A scale of hours associated with the development of the tissues reaction to a foreign body (the electrode).

To connect variables that belong to this time scales with variables of interest in a given reference scale, the variables in the slower scales can be considered as fixed parameters and

the variables in the faster scales can be considered relaxed to equilibrium in the scale of reference. [3] So, between a pacing pulse and the next one the distance between the electrodes and the target tissue could be modified due to muscle contraction. However, during the interval of application of a given pulse, in the scale (b), this distance can be considered as fixed, because all the modifications in the capsule of fibrous tissue that surrounds the electrode's head occur in the time scales (c) and (d).

(B) The two media hypothesis and the coupling between the two continua

It is advisable to split the part of the electric subsystems belonging to the excitable myocardium in two superposed conductors of electricity:
One conductor (let us call it the red continuum) is formed by the excitable membranes of the active electric subsystem.
The other conductor (let us call it the blue continuum) is formed by the intracellular and the interstitial spaces of the passive electric subsystem combined in a volume conductor and electrically connected through the cellular membranes. Figure 3 shows an abstract representation of these continua.

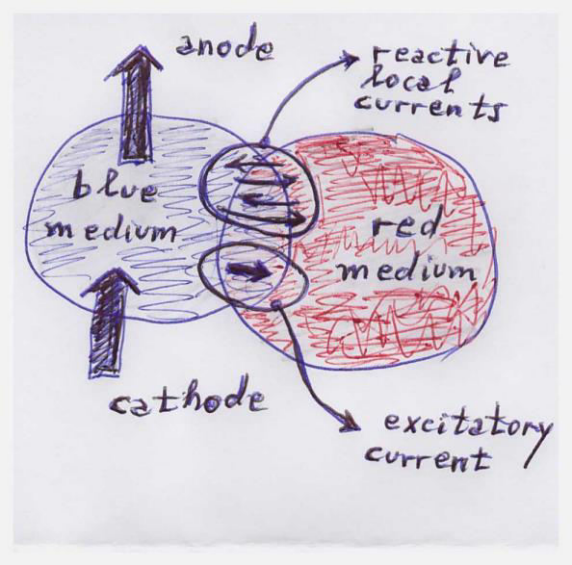

Figure 3: The two idealized continua.

According to this approach, each point in the excitable myocardium belongs to both continua. [4]

[3] A more detailed discussion of these simplifying principles can be found in (H) 8, (H) 9 and (H) 10.

[4] This was developed by Tung and other authors as the bidomain model of electrocardiology. (See H (6) and H (21)).

To obtain an operational (constructive) procedure of homogenization suitable to this case, the method of volume averaging already employed in the study of transport processes in porous media (G (18)) could be applied[5]. Meanwhile, a postulation approach allows write a pair of coupled equation for the red and blue continua in time t and space $\vec{r}$.

Considered as the abovementioned red continuum, the excitable membranes of the heart could be represented by a space filling three-dimensional nonlinear cable (a simplified isotropic and homogeneous version appears in G (8)).
The blue continuum is anisotropic, and as shown in G (2), the anisotropy is different (unequal anisotropy) in the intracellular space relative to the interstitial space. This must be taken into account in the mathematical model.

If $V_m(t,\vec{r})$ is the field of membrane voltage (potential inside minus potential outside), a state variable of the red continuum, and if R_x, R_y, R_z represent certain electric resistances per unit length in the direction of suitable chosen coordinate axis, assuming homogeneity (albeit unequal anisotropy) and other convenient assumptions, it seems possible to write the following approximate equation to connect the current density **per unit volume** across the excitable membranes I_m with an exogenous current density **per unit volume** I_{ex} and with a density **per unit volume** of reactive currents associated with the non-uniformity of the polarization of the excitable membranes due to the active electrode: [6]

$$I_m = I_{ex} + \frac{1}{R_x}\cdot\frac{\partial^2}{\partial x^2}V_m + \frac{1}{R_y}\cdot\frac{\partial^2}{\partial y^2}V_m + \frac{1}{R_z}\cdot\frac{\partial^2}{\partial z^2}V_m \qquad (1)$$

Currents are taken as positive when they flow from the intracellular space towards the extracellular (interstitial) space.

---

[5] A foundation of bidomain model using the theory of averaged fields is given in H (9). A different foundation of the homogeneization procedure, using perturbation theory, is given in H (5).

[6] **Introducing the fraction χ_m of membrane area per unit volume, the density of membrane current per unit area J_m can be related with the density $\vec{J}(t,\vec{r})$ of electric current in the tissue's volume conductor by $\chi_m \cdot J_m = \nabla \bullet \left(\widetilde{C} \bullet \nabla V_m\right) + \nabla \bullet \left(\widetilde{D} \bullet \vec{J}\right)$. As usual, ∇ represents the gradient operator and $\bullet$ represents the scalar product. The tensor field $\widetilde{C}$ is symmetric and positive definite. It is related with a tensor generalization of the known scalar cable space constant. The symmetric tensor field $\widetilde{D}$ depends on the electrical properties of the blue continuum. The term $\nabla \bullet \left(\widetilde{D} \bullet \vec{J}\right)$ is equivalent to Rattay's activating function of a nerve or skeletal muscle fibre. See H (9), H (10), H (18), H (19), H (20) and H (21).**

We further assume that the blue continuum can be modelled as an anisotropic and Ohmic volume conductor. Applying the quasi-stationary equations of electromagnetics, it should be expected the following factorization:

$$I_{ex}(t,\vec{r}) = i(t)\cdot F_I(\vec{r}) \tag{2}$$

The membrane current is the sum of a displacement current $C_{m,V}\cdot\frac{\partial}{\partial t}V_m$ (here $C_{m,V}$ is an electric capacitance of excitable membranes per unit volume) with an ionic current $I_{ion}(V_m,\vec{W})$, where the vector $\vec{W}$ completes the set of state variables of the red continuum and embraces activation, recovery and other even slower variables related with the ionic channels.

To simplify the analysis, it will be assumed that the activation variables are relaxed to equilibrium with membrane voltage, and the recovery variables will be considered as frozen. Then the ionic current $I_{ion}(V_m)$ behaves as shown in Figure 4, being positive for membrane voltages between V_R (the rest membrane voltage, a first zero of the ionic current) and V_{Th} (the uniform membrane threshold, a second zero of the ionic current), and negative between V_{Th} and the excited state voltage V_E (this last zero of the ionic current is a consequence of the freezing of recovery variables).

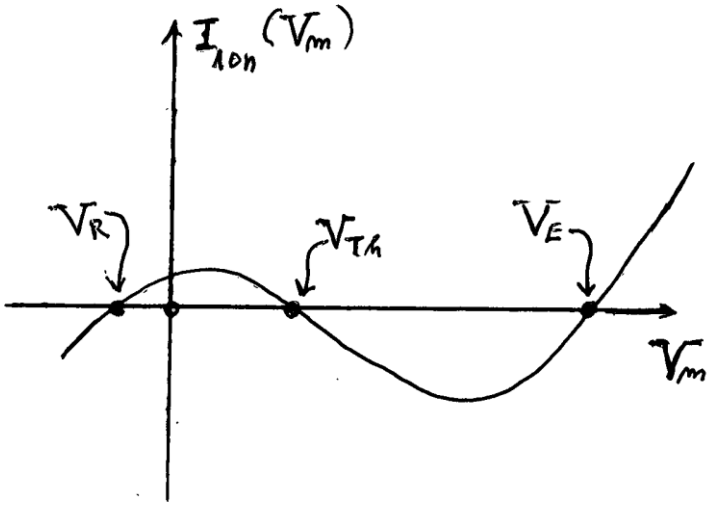

Figure 4: Sketch of the ionic current per unit volume of the red continua (excitable membranes) as a function of membrane voltage for activation variables relaxed to equilibrium and recovery variables frozen.

Considering the above mentioned two terms in the membrane current, equation (1) can be re-casted as follows:

$$C_{m,V}\cdot\frac{\partial}{\partial t}V_m = -I_{ion}(V_m) + \frac{1}{R_x}\cdot\frac{\partial^2}{\partial x^2}V_m + \frac{1}{R_y}\cdot\frac{\partial^2}{\partial y^2}V_m + \frac{1}{R_z}\cdot\frac{\partial^2}{\partial z^2}V_m + I_{ex}(t,\vec{r}) \tag{3}$$

(C) The treshold condition at membrane level

After the end of a stimulating cathodic pulse the excitable membranes of a region located near the electrode are polarized due to the external current field. The space-time evolution of membrane voltages between stimulating pulses will be described by:

$$C_{m,V} \cdot \frac{\partial}{\partial t} V_m = -I_{ion}(V_m) + \frac{1}{R_x} \cdot \frac{\partial^2}{\partial x^2} V_m + \frac{1}{R_y} \cdot \frac{\partial^2}{\partial y^2} V_m + \frac{1}{R_z} \cdot \frac{\partial^2}{\partial z^2} V_m \qquad (4)$$

According with Rushton, in the case of a nerve fibre, or according to Fozzard and Schömberg, in the case of a Purkinje fibre, in order to produce an action potential **a liminal length of fibre must be depolarized above the uniform membrane threshold**. A detailed study and justification can be found in G (8).

Ventricular myocardium behaves as an electric syncytium. Lindeman's experimental results about thresholds of stimulation of ventricular myocardium by external electrodes (G (14)) can be explained assuming that **an action potential is produced if the membranes of a suitable three dimensional region are depolarized above the uniform membrane threshold** V_{Th}**.** In principle the analysis given in Chapter 12 of G (8) could be extended from

a one dimensional nonlinear cable to a three dimensional one, and a derivation of the size and shapes of liminal regions obtained. [7]

An heuristic approach to the liminal region could be this. Let us consider the more depolarized point with voltage V_M and develop the ionic current $I_{ion}(V_m)$ in a neighborhood of V_{Th} to the first order in $V_M - V_{Th}$.

Applying a similar procedure as, for example, the one explained by Kyrala (G (10)) to get an interpretation of the Laplacian of a scalar field in a reference point in space, approximate the spatial second derivatives of voltage $\frac{\partial^2}{\partial x^2} V_m$ by $-\frac{V_M - V_{Th}}{l_x^2}$, $\frac{\partial^2}{\partial y^2} V_m$ by $-\frac{V_M - V_{Th}}{l_y^2}$ and $\frac{\partial^2}{\partial z^2} V_m$ $-\frac{V_M - V_{Th}}{l_z^2}$, all of them in the most depolarized point. The lengths l_x, l_y and l_z measure the distance between the most depolarized point and the points, located on the x, y, and z axes, where the membrane voltage is at its uniform threshold. They characterize the size and shape of **an influence region of the electrode on the excitable tissue**.

Equation (4) is the approximated at the most depolarized point by:

$$C_{m,V} \cdot \frac{\partial}{\partial t} V_M \approx \left(\left| \frac{\partial}{\partial V_m} I_{ion}(V_{Th}) \right| - \left(\frac{1}{R_x \cdot l_x^2} + \frac{1}{R_y \cdot l_y^2} + \frac{1}{R_z \cdot l_z^2} \right) \right) \cdot (V_M - V_{Th}) \qquad (5)$$

[7] **A full analytical approach to the characterization of liminal regions can be found in references H (9), H (10), H (14), H (18), H (19), and H (20).**

From equation (5), if $\left|\frac{\partial}{\partial V_m} I_{ion}(V_{Th})\right|$ is greater (smaller) than $\frac{1}{R_x \cdot l_x^2}+\frac{1}{R_y \cdot l_y^2}+\frac{1}{R_z \cdot l_z^2}$ the voltage V_M should increase (decrease). We could suspect that in the first case excitation will succeed and in the other it will fail. If the size of the influence region is too small, the excitation should fail. **But all this lacks enough rigor.**

In any case we can guess that when the depolarization is more localized, its value in the most depolarized point should be greater, and the always negative term $\frac{1}{R_x}\cdot\frac{\partial^2}{\partial x^2}V_m+\frac{1}{R_y}\cdot\frac{\partial^2}{\partial y^2}V_m+\frac{1}{R_z}\cdot\frac{\partial^2}{\partial z^2}V_m$ related with the reactive currents there would be greater in absolute value. As consequence, we could guess that other circumstances equal, the threshold cathodic pulse amplitude will be greater also.
If this is so, it seems that **to lower current threshold it would be advisable to depolarize as uniformly as possible the target region in excitable myocardium**. An more uniform depolarization could be reached with a constant field electrode. To assess what could be attainable in practice, let us consider now the geometry of the current fields produced near the head of an active cathode.

(D) Geometry of the exogenous electric current field in tissue's volume conductor

Let us consider a metallic cathode of any shape immersed in a volume conductor.
Under quasi-steady conditions the field of electric current density $\vec{J}$ is solenoidal (divergence free): $$\nabla \bullet \vec{J} = 0 \qquad (6)$$
If $\vec{t}$ is the tangent unitary vector to a field line Γ in the point P then, with $J = \left\|\vec{J}\right\|$ being the local field magnitude (norm): $$\vec{J} = J \cdot \vec{t} \qquad (7)$$
From (6) and (7) it follows: $$\nabla \bullet \vec{J} = \vec{t} \bullet \nabla J + J \cdot \nabla \bullet \vec{t} = 0 \qquad (8)$$

The gross point $\bullet$ represents the scalar product of two vectors, $\nabla \bullet (\ )$ represents the divergence operator and $\vec{t} \bullet \nabla J = \frac{dJ}{ds}$ is the directional derivative of the current density magnitude along the field line of intrinsic abscissa s (arc length) (G (1) and G (4)).
Let us further assume that the volume conductor is isotropic. Then the unit vector $\vec{t}$ is at the same time tangent to a field line at a point P and a normal unitary vector to the equipotential surface crossed by the field line at the same point P (see Figures 5 and 6).
There is a relation between the divergence of the field of normal unit vectors and the mean curvatures H of the equipotential surfaces at the same point (G (1), G (4) and G (9)). **With a suitable sign convention for the mean curvature**, it can be written thus:

$$\nabla \bullet \vec{t}(P) = -2 \cdot H(P) \qquad (9)$$

From equations (8) and (9) it is possible to show that current densities magnitudes $J(P)$ and $J(Q)$ at any two points P and Q over the same field line Γ (see Figure 5) are related by a functional of the mean curvatures H_Γ (also known as Germain's curvature) of the points of the equipotential surfaces crossed by said field line between these two points:

$$\frac{J(Q)}{J(P)} = \exp\left[2 \cdot \int_{s_P}^{s_Q} H_\Gamma(s) \cdot ds\right] \tag{10}$$

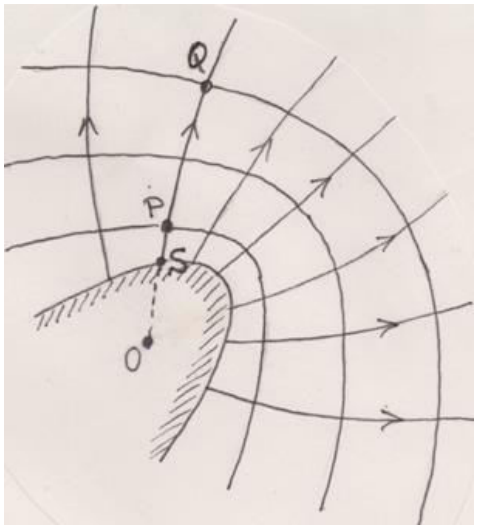

Figure 5: A planar sketch of field lines and equipotential surfaces for a convex electrode.

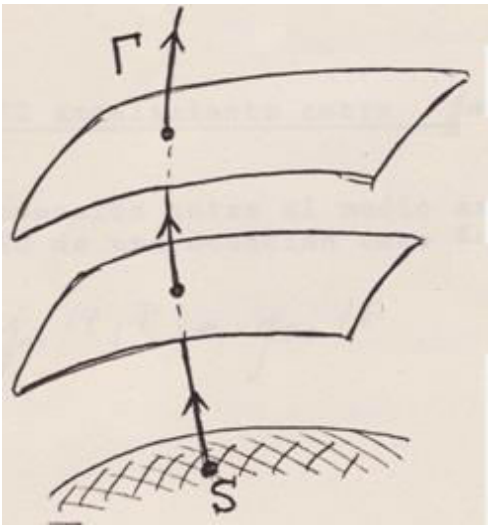

Figure 6: A three-dimensional sketch of field lines and equipotential surfaces.

The point O that appears in the interior of the cathode material in figure 5 is the **electric centre of the electrode**. The electric centre is such that taking it as origin of the position vectors $\vec{r}$, the following equation is verified:

$$\int_{\partial B} \left(\vec{J} \bullet \vec{n}\right) \cdot \vec{r} \cdot dS = \vec{0} \tag{11}$$

In this formula the normal component $\vec{J} \bullet \vec{n}$ of the electric current density at a point in the surface of the electrode head is multiplied by the position vector of this point and the result is integrated on the entire electrode surface.

From now on it is assumed that the conductivity of the electrode material (for example, Platinum) is at least an order of magnitude greater than the conductivity of the tissues.

A good approximation is to consider that the conducting electrode surface is an equipotential surface and that the field lines are orthogonal to the electrode surface when the volume conductor behaves isotropically.

Figure 7 shows a sketch of a concave electrode and its field of current lines, for an unbounded, homogeneous, and isotropic volume conductor. Some asymptotes are sketched also.

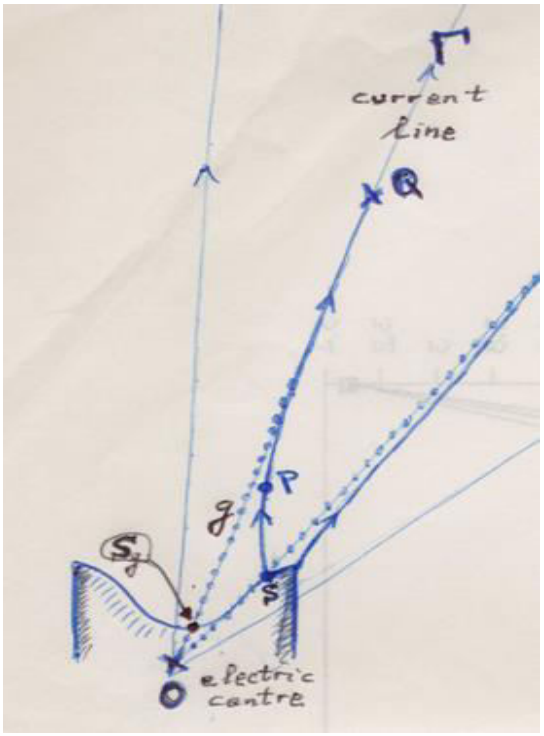

Figure 7: The field lines Γ are asymptotic to straight lines g that pass through the electric centre O of the electrode. The field line begins in a point S on the electrode surface that is in general different from the point S_g where the line g crosses the surface of the electrode.

When the curvilinear abscissa s grows, the magnitude of the electric current density $J(P)$ approaches the result corresponding to a point electrode: $\dfrac{i(t)}{4\cdot\pi\cdot(0S_g+s_P)^2}$

Let us introduce **the excess mean curvature of an equipotential surface relative to a spherical surface** constructed using the asymptote g :

$$\Delta H(s)=H(s)-\frac{1}{(0S_g+s)^2} \tag{12}$$

From Equation (10) and (12) we derive a formula for the magnitude of the electric current density in any point P as a functional of the excess mean curvature integrated on a half field line beginning at P and extending to infinitum:

$$J(P) \approx \frac{i(t)}{4 \cdot \pi \cdot (0S_g + s_P)^2} \cdot \exp\left[-2 \cdot \int_{s_P}^{+\infty} \Delta H(s) \cdot ds \right] \qquad (13)$$

The generalization of formula (12) to the case of an anisotropic volume conductor will be considered elsewhere, applying some results obtained by Morris Kline (G (9)) to a problem of geometrical optics. However, the formula as it is by now should be enough for the purposes of this paper, centred in a qualitative discussion.

(E) The possibility of a constant field electrode: the concept of an electrode's critical region

There is a theorem of classical vector field theory (due to Prim, see G (15)) that allows us to pose the type of electrode that is needed to make more uniform the polarizing effect of the cathode (the constant field electrode).
According to it, for regular enough complex lamellar fields (fields that are equal to the product of a gradient field by a scalar field) the following three statements are equivalent:

1- The surfaces orthogonal to the field are minimal surfaces (the mean curvature vanish at each point).
2- The field is divergence free.
3- The field magnitude is constant along each field line.

A infinite Platinum half space electrode with a planar interface separating it from a complementary infinite half space filled with an ohmic, homogeneous and isotropic volume conductor produces a constant field everywhere, but is not attainable in practice.
Nevertheless, a concave electrode like the one already sketched in Figure 7, shows several very interesting properties.

Figure 8 sketches the behaviour of the magnitude of the electric current density $J(P)$ along a field line located near a cathode axis of symmetry, given as a
function of the intrinsic abscissa s with the origin in the interface between the electrode and the tissues.

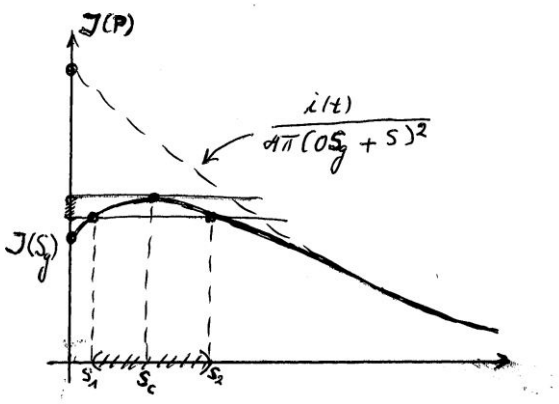

Figure 8: A sketch of the modification of the magnitude of the electric current density along a current line.

The magnitude of the current density remains nearly constant along a segment of field line where the mean curvatures change their sign (the mean curvature in s_c is exactly zero, being negative before and positive after it, according to the sign convention chosen here). An interval (s_1, s_2) can be constructed such that inside it the mean curvatures remain in absolute magnitude less than a pre-established small number and the distance between the magnitude of the current density and its maximum value $J(s_c)$ remains less than a corresponding small number.
Thus, it seems that a **critical region** will be produced, located at some distance from the cathode surface, where the field lines will be relatively parallel, and the magnitude of the current will be higher than in its neighbourhood.

The assessment of the feasibility of designing, constructing and implanting an electrode with these advantages ("jumping" over the capsule of non-excitable tissues, lowering the electrochemical polarization of the double layer in the interface between the electrode and the tissues, and generating a critical region with suitable shape and size to lower the stimulation threshold counteracting the effect of the physiological increase) deserves a deeper study, both theoretical and experimental, with animal models and clinical trials.

Merely as suggestions to begin with, Figure 9 shows two tentative electrode shapes.
It is possible to anticipate that the one that appears in the left should show too much electrochemical polarization in the high curvature edges that surround the concavity.

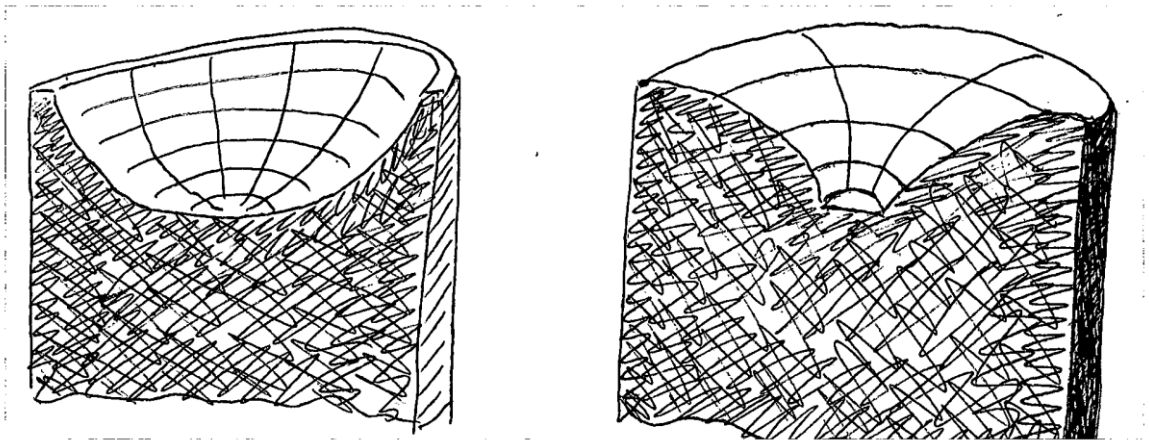

Figure 9: Examples of possible electrode shapes.

(F) Acknowledgements

To Eng. Carlos A. Leguizamón, head of the joint Biomathematics Group of the Atomic Energy Commission of Argentina and the Department of Mathematics, School of Natural and Exact Sciences, Buenos Aires University, for his support and encouragement.

II International Congress of Biomathematics

Buenos Aires, Argentina September 14, 1984

To Dr. Orestes Fiandra M. D., who since 1979 has been guiding the author through the complexities of electro-cardiology and artificial cardiac pacing.

(G) Bibliography

1. Brand, L. "*Vector and tensor analysis*", Mc Graw-Hill, New York, 1947.

2. Chapman, R. and C. Fry, "An analysis of the cable properties of frog ventricular myocardium", *J. Physiol*. **283**, pp. 263-282, 1978.

3. Christer, J. Sylvén H. and others, "Pacing Threshold interval with decreasing and increasing output", *PACE*, **5**, pp. 646-649, 1982.

4. Ericksen, J. "*Tensor Fields*", Appendix to Truesdall C. and R. Toupin, "*The classical field theories*", Encyclopedia of Physics, volume 3, Springer, Berlin, 1960.

5. Fiandra, O. Suárez Antola, R. and others, "Endocardic stimulation. Observations after the implant of permanent leads", *Estimulación Cardíaca*, **2** (4), pp. 209-, 1981.

6. Flügge, W. "*Viscoelasticity*", Springer, Berlin, 1975.

7. Fozzard, H. "Conduction of the Action Potential" in *Handbook of Physiology*, *The Cardiovascular System I*, pp. 335-356, 1979.

8. Jack, J. Noble D. and R. Tsien, "*Electric current flow in excitable cells*", Clarendon Press, Oxford, 1975.

9. Kline, M. "A note on the expansion coefficient of geometrical optics", *Comm. Pure Appl. Math.*, **14**, pp. 473-479, 1961.

10. Kyrala, A. "*Theoretical Physics: Applications of vectors, matrices, tensors and quaternions*", William Saunders, Philadelphia, 1967.

11. Irnich, W. "The chronaxie time and its practical importance", *PACE*, **3**, pp. 292-301, 1980.

12. Irnich, W. "Comparison of pacing electrodes of different shape and material: recommendations", *PACE,* **6**, 422-426, 1983.

13. Laplantif, J. "*Importance de la geometrie des electrodes dans la valeur du seuil aigu de stimulation cardiaque*", Ph. D. Thesis, Poitiers, 1983.

14. Lindemans, F., "*Electrical stimulation of heart muscle*", Ph.D. Thesis, Uthretch: Elinkwijk, 1977.

15. Prim, R. "On doubly laminar flow fields having a constant velocity magnitude along each stream-line", U.S. Naval Ordnance Lab. Memoir Nº 9762.

16. Schaldach, M. y S. Furman (Editors) "*Advances in pacemaker technology*", Engineering in Medicine 1, Springer, Berlin, 1975.

17. Santaló, L. "*Vectores y Tensores con sus Aplicaciones*" Eudeba, Buenos Aires, 1977.

18. Slattery, J. "*Momentum, energy and mass transfer in continua"*, McGraw-Hill Kogakusha, Tokyo, 1972.

19. Suárez-Ántola, R. "*Bio-mathematical perspectives of chronic cardiac pacing*", DPE, Universidad de la República, Montevideo, Uruguay, 1983. In Spanish.

20. Suárez Antola, R. "*An application of vector field theory to the analysis of erosion siphoning*" (*Una aplicación de la Teoría de los Campos Vectoriales Solenoidales Casi Gradientes al análisis del Sifonaje por Erosión*), DPE, Universidad de la República, Montevideo, Uruguay. To be published in October 1984. In Spanish.

21. Talbot, S.A. and U. Gessner "*Systems physiology*", Wiley, New York, 1973.

(H) Additional bibliography, related with the content of the present paper, and published after its oral presentation:

1. Aubert, A. and H. Hector (Editors) "*Pacemakers leads*", Elsevier, Amsterdam, 1985.

2. Fiandra, O. and others, "*Cardiac Pacemakers*", Department of Cardiology (School of Medicine, Universidad de la República) and National Institute of Cardiac Surgery, Montevideo, 1985. ISBN 84-89266-00-X. In Spanish.

3. Fiandra O. and others, "The cathode in cardiac stimulation: influence of its shape in chronic thresholds", *Annals of the VII Uruguayan Congress of Cardiology*, Montevideo, 1985. In Spanish.

4. Fiandra O. and R. Suárez-Antola, "*Electrode for electric stimulation of living tissues*", *UY*- Patent *12.817*, Montevideo, 1987. In Spanish.

(Available in https://www.researchgate.net/profile/Roberto_Suarez-Antola/?ev=hdr_xprf)

5. Henriquez, C., and W. Ying "The bidomain model of cardiac tissue: from microscale to macroscale", Chapter 5.1 in I. Efimov, M. Kroll y P. Tchou (Eds.) "Cardiac bioelectric therapy", New York, Springer, 2009.

6. Janks, D. and B. Roth "The bidomain theory of pacing", Chapter 2.1 in I. Efimov, M. Kroll y P. Tchou (Eds.) "Cardiac bioelectric therapy", New York, Springer, 2009.

7. Suárez Antola R. "Una aplicación de la Teoría de los Campos Vectoriales Solenoidales Casi Gradientes al análisis del Sifonaje por Erosión", DPE, UDELAR, 1984. DOI: 10.13140/2.1.4801.1201

8. Suárez Antola, R. "*Biomathematical outlooks of chronic cardiac pacing*", Chapter 8 in Fiandra, O. and others, "*Cardiac Pacemakers*", Department of Cardiology (School of Medicine, Universidad de la República) and National Institute of Cardiac Surgery, Montevideo, 1985. In Spanish. (There is an English translation of this chapter made by request of Dr. Seymour Furman). DOI: 10.13140/2.1.1655.3926

9. Suárez Antola R. "*Biophysical foundations for the study of electric excitation and action potential propagation in myocardium*", M. Sc. Thesis, PEDECIBA, UdelaR, Montevideo, 1991. DOI: 10.13140/2.1.4211.2962

10. Suárez-Ántola, R. "*Thresholds: Contributions to the study of excitation and propagation of the electric activity of biological tissues stimulated by external electrodes*", D.Sc. Thesis, PEDECIBA, UdelaR, Montevideo, 1994. In Spanish. DOI: 10.13140/2.1.2572.8968

11. Suárez-Ántola, R. Griego, J. and O. Fiandra, "Concave Electrodes I: Experimental Foundations". *Physics in Medicine and Biology*, **39**, 1994.

(Extended summary available in https://www.researchgate.net/profile/Roberto_Suarez-Antola/?ev=hdr_xprf)

12. Suárez-Antola, R. "Concave Electrodes II: Theoretical Foundations", *Physics in Medicine and Biology*, **39**, 1994.

(Extended summary available in https://www.researchgate.net/profile/Roberto_Suarez-Antola/?ev=hdr_xprf)

13. Suárez-Antola, R. and G. Artucio, "Concave Electrodes III: Computer Assisted Design", *Physics in Medicine and Biology*, **39**, 1994.

(Extended summary available in https://www.researchgate.net/profile/Roberto_Suarez-Antola/?ev=hdr_xprf)

14. Suarez-Antola, R. "Outline of an analytical approach to threshold dynamics for excitable tissues stimulated by external electrodes" in "Modeling the Heart", *Fifth Conference of the European Society for Engineering and Medicine*, Barcelona, Spain, 1999.

15. Suarez-Antola, R. "The time constants for cathodic make stimulation of electrical syncytia: an application to cardiac pacing", *Proceedings of the 2006 Conference of the IEEE Engineering in Medicine and Biology Society*, 4031-4034, 2006.

16. Suárez-Ántola, R. "Sensing bioelectric signals with concave electrodes: I. Lead fields and sensitivity", *Revista Iberoamericana de Sensores*, 5 (2), 2006. ISSN 9974-0337.

17. Suárez-Antola, R. "Sensing bioelectric signals with concave electrodes II: Experimental and analytical approaches to electrode design", *Revista Iberoamericana de Sensores*, **6** (1), 114-121, 2008. ISSN 9974-0337.

18. Suárez Ántola, R. "A Nonlinear Modal Analysis of Threshold Dynamics for Cardiac Tissue Excited by External Electrodes", Annual Meeting of the German Biophysical Society, (Section III: Medical Biophysics), Göttingen (DE), 2012. DOI: 10.13140/2.1.2413.0566

19. Suárez Ántola, R. "Modelo fisicomatemático de la dinámica del umbral de estimulación eléctrica del miocardio mediante electrodos de marcapaso. Parte I: Sincicio eléctrico isótropo y homogéneo", Rev. SCP, Tercera Época, volumen 18, Nº 2, pp.145-174, 2013. ISSN 0379-9123
(Available in https://www.researchgate.net/profile/Roberto_Suarez-Antola/?ev=hdr_xprf)

20. Suárez Ántola, R. "Modelo fisicomatemático de la dinámica del umbral de estimulación eléctrica del miocardio mediante electrodos de marcapaso. Parte II: Sincicio eléctrico anisótropo y heterogéneo", Rev. SCP, Tercera Época, volumen 19, Nº 2, pp.135-168, 2014. ISSN 0379-9123
(Available in https://www.researchgate.net/profile/Roberto_Suarez-Antola/?ev=hdr_xprf)

21. Tung, L. "The generalized activating function", Chapter 2.3 in I. Efimov, M. Kroll y P. Tchou (Eds.) "Cardiac bioelectric therapy", New York, Springer, 2009.

22. Walton, C. Gergely, S. and A. Economides, "Platinum pacemaker electrodes: origins and effects of the electrode-tissue interface impedance", *PACE*, **10**, 87, 1987.

Physics in Medicine and Biology, vol. 39 a, 1994

CONCAVE ELECTRODES I: EXPERIMENTAL FOUNDATIONS

Roberto Suárez Ántola[(1)], Jorge Griego[(2)] and Orestes Fiandra[(3)]

[(1)] Asesor, Dirección Nacional de Tecnología Nuclear, Ministerio de Industria, Energía y Minería.
[(2)] Profesor Agregado, Facultad de Ciencias, Universidad de la República.
[(3)] Director del Centro de Construcción de Cardioestimuladores y antiguo Profesor Director del Departamento de Cardiología, Facultad de Medicina, Universidad de la República, Montevideo, Uruguay.

Introduction The shape and size of electrode's head have a strong influence both on acute and chronic pacing threshold and sensing performance when target's region is close enough to electrode's surface. This is particularly relevant to myocardial pacing, but besides that, it may be of interest for pacing of nervous system and skeletal and smooth muscle.

Materials and Methods (a) Fields generated by seven model electrodes, of the same size and material composition but different shapes, were studied from an experimental point of view using an electrolytic tank. The equipotential surfaces surrounding each electrode were measured in steady state, for hemispherical, conventional cylindrical and five shapes of concave electrodes, in order to make a comparison of the resultant fields. (b) After that, a shape of concave electrode (named by us "clothoidal") was selected and a real size platinum electrode was made with it. Then, it was implanted together with a conventional cylindrical platinum electrode, in the myocardium of ten dogs. The strength-duration curve for each electrode was measured in each dog, once a day, during several weeks. Rheobases, chronaxies and limit threshold charges were determined from experimental data.

Results and Conclusions (a) A region located at a significant distance from electrode's surface is formed, for special concave electrode (clothoidal), where current density is higher and current lines are relatively parallel (**critical region of the electrode**). (b) At implant, the strength-duration curve for the conventional electrode was under the strength-duration curve for the clothoidal electrode. But after several days the situation suffered an inversion, mainly because conventional rheobases began to grow significantly meanwhile clothoidal rheobases didn´t grew so much, maintained its acute values **or even decreased**.

Key words: concave electrodes, clothoidal electrodes, critical region, stimulation thresholds, cardiac pacing, electrolytic tank experiments, scale models, rheobas, chronaxie, limit threshold charge.

Physics in Medicine and Biology, vol. 39 a, 1994

EXTENDED SUMMARY

(A) Introduction

The shape and size of electrode's head have a strong influence both on acute and chronic pacing threshold and on the sensing performance of the electrode, when the target region is close enough to the surface of the electrode (Irnich, 1980; Laplantif, 1983; Suárez-Antola, 1983; Fiandra el alt, Chapters 7 and 8, 1985 a; Fiandra et alt, 1985 b; Aubert and Hector, 1985). This is particularly relevant to myocardial pacing, but besides that, it may be of interest for pacing of nervous system and skeletal and smooth muscle.

The influence of the size and shape of the head of the electrode is due to the geometry of the electric current field generated by the electrode in the volume conductor formed by the biological tissues, and to the position of the target region (when pacing) or of the signal source (when sensing) in this volume conductor.

In concave electrodes a certain **critical region**, where current density is higher and field lines are relatively parallel, is produced at a certain distance from electrode's surface (Fiandra and Suárez-Antola, 1987). The present experimental work affords some evidence that suggests an improvement of the pacing performance in a particular case of concave electrode, named clothoidal electrode, relative to other cardiac pacing electrodes.

(B) Materials and Methods

Fields of electric potential and current generated by seven giant model electrodes, of the same size (0.03 m diameter and 0.03 m height) and material composition (aluminium) but different shapes, were studied using an electrolytic tank (1 m diameter and 0.8 m height).

The electrode's shapes, all with cylindrical symmetry (in fact, flat meridian symmetry), are shown in vertical cross section in Figure 1: a hemispherical electrode, a plane electrode, two concave hemispherical electrodes (with arrows 0.004 m and 0.0085 m), two clothoidal electrodes (with arrows 0.0137 m and 0.0170 m) and a hemispherical concave electrode with rounded borders.

Figure 2 shows the measurement system: the tank (T) filled by an watery electrolytic solution (CV, homogeneous and isotropic volume conductor), the working electrode (R) mounted on an isolating cylinder (S) centred in the tank's axis (e), the counter electrode (made of an aluminium foil of very large area), stick to the inner side of the vertical wall of the tank, a measuring electrode (E) (a slender pipette mounted in a mechanical systems that allows both horizontal and vertical displacements, and filled with a KCl solution surrounding a thin wire of Ag-AgCl), a voltage source and a voltmeter. A controlled (from 0 to 9V) voltage source (F) was connected between the working and the indifferent

electrode as shown in Figure 2. The local voltage between the measuring electrode and earth was determined with a Hewlett-Packard multimeter (V).

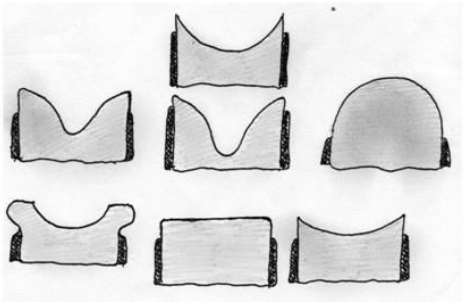

Figure 1: Vertical cross sections of the electrodes

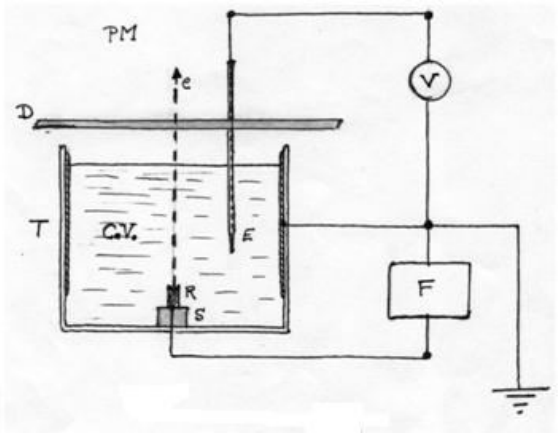

Figure 2: Electrical measurement system.

A specific shape of clothoidal-concave electrode was chosen after analysing the results of the experiments done with the above mentioned electrolytic tank.

Figure 3 shows in cross section the chosen shape for the clothoidal electrode used in the threshold experiments done in dogs. From this template, a special cutting tool was made in Barcelona, Spain, to be applied in a jeweler's lathe to obtain the desider concavity in one of the circular faces of a platinum cylinder.

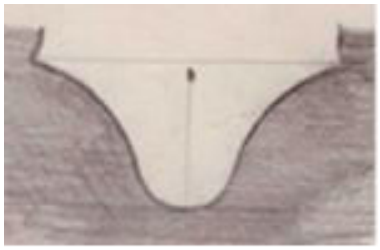

Figure 3: Template of a clothoidal electrode

Real size clothoidal porous platinum electrodes were hand crafted by Dr. O. Fiandra (M. D.) in his jeweler's lathe.

The clothoidal electrodes were implanted, together with a conventional cylindrical porous platinum electrode of the same size (2 mm diameter), in the myocardium of ten dogs. The strength-duration curves for each electrode were measured in each dog, once a day, during several weeks. Rheobases, chronaxies and limit threshold charges were determined from experimental data. Only some threshold values are reported here. The detailed experiments as well as a complete and in depth analysis of the obtained results will be presented elsewhere.

During all threshold measurements, intracavity electrocardiograms were registered from both electrodes in order to compare their sensing capabilities.

Figures 4 to 6 shows one of the real size clothoidal electrodes implanted in a dog's heart.

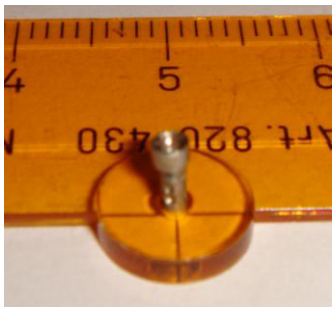

Figure 4

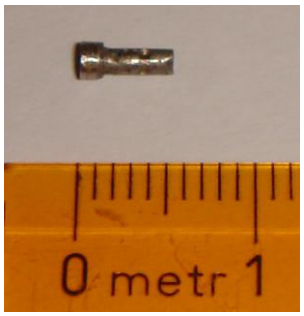

Figure 5

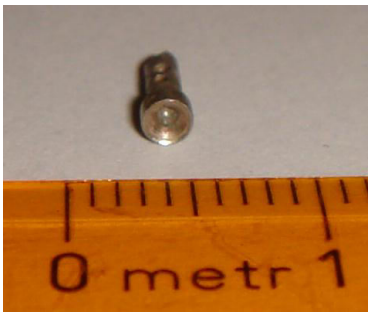

Figure 6

(C) Results

(C.1) The equipotential curves sketched in Figures 6 to11 were determined in steady state. We didn't find significant differences in the equipotential surfaces determined with 60 Hz AC relative to the same surfaces determined using DC. The equipotential curves of the hemispherical electrode are not shown because they correspond very closely to hemispheres at all distances from electrode's surface, with the only exception of the region below the horizontal plane that passes through the electrode's centre. This region has no interest, neither for pacing nor sensing.

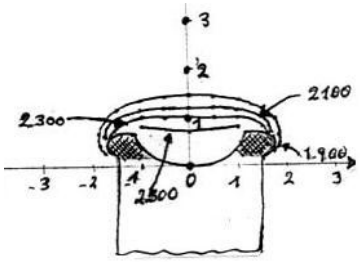

Figure 6

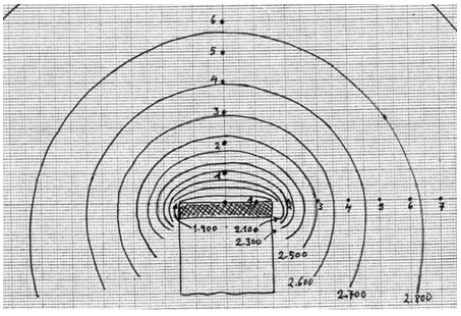

Figure 7

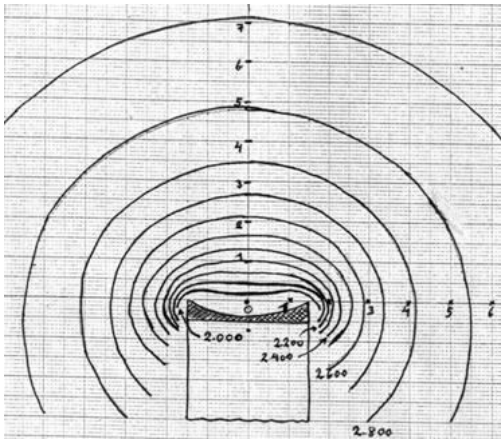

Figure 8

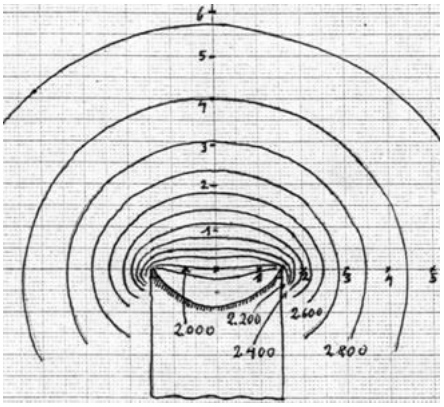

Figure 9

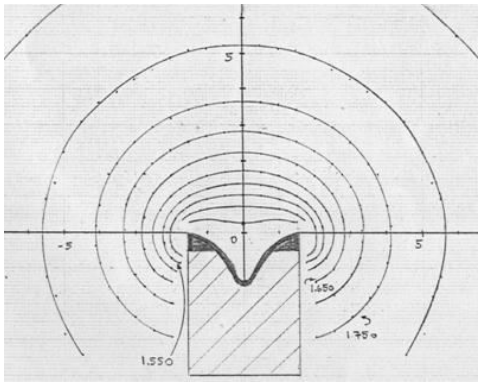

Figure 10

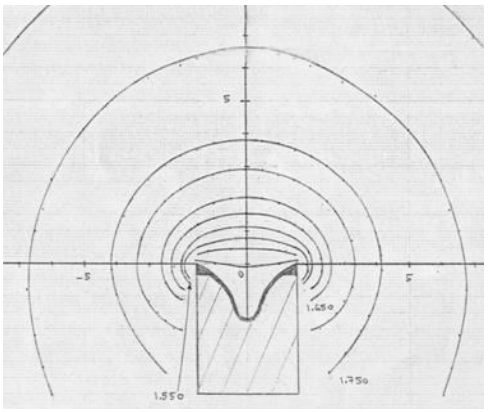

Figure 11

The electric potential difference between adjacent curves is the same in all cases, so that the reciprocal of the distance between curves gives a measure of the magnitude of the electric field. Due to the fact that the volume conductor behaves as homogeneous and isotropic, this reciprocal distance also can be taken as a measure of the local electric current density.

As can be seen exemplified in Figures 7 to 11, in the concave electrodes case, a particular region centred on the axis of symmetry and located at a certain distance from electrode's surface is formed. For all electrodes the electric potential decreases monotonically along the axis of symmetry. But for concave electrodes the potential shows an inflection point where the magnitude of the electric field (and as consequence, the magnitude of the electric current density) is a maximum. In a neighbourhood of this point the magnitude of the electric current density is higher and the current lines near the axis are relatively parallel.

This region can be named the **critical region of the electrode**. This critical region is both, farther away (from electrode's surface) and bigger, for clothoidal electrodes in comparison with other concave electrodes of the same size and material.

(C.2) Now we show the rheobase, the chronaxie and the limit threshold charge calculated from the measured strength-duration curves in two dogs (D-4 and D-5) both for the clothoidal (α) and the conventional (β) porous platinum electrodes. The data correspond to the implantation of the electrodes (time 0), and then to the first (time 1), the fourth (time 4), and the eight (time 8) day after the implant.

D-4

		Time 0	Time 1	Time 4	Time 8
Rheobase	α	0.20	0.71	0.71	0.72
(mA)	β	0.49	0.68	1.12	1.13
Chronaxie	α	0.54	0.36	0.21	0.38
(ms)	β	0.35	0.15	0.29	0.30
Limit Threshold	α	0.11	0.25	0.22	0.27
Charge	β	0.17	0.10	0.32	0.34

D-5

		Time 0	**Time 1**	**Time 4**	**Time 8**
Rheobase	α	0.64	1.22	0.84	0.81
(mA)	β	0.39	1.05	1.55	2.15
Chronaxie	α	0.27	0.21	0.17	0.49
(ms)	β	0.21	0.24	0.15	0.31
Limit Threshold	α	0.17	0.26	0.14	0.40
Charge	β	0.08	0.25	0.23	0.67

The rheobases behave according to the physiological increment of the threshold of excitability of myocardium (Fiandra and others, 1985 a, Chapter 7; Fiandra, Suárez-Antola and others, 1981).

In D-4 and D-5, as well as in the other dogs, the rheobases of the clothoidal electrodes increased less than the rheobases of the conventional electrodes. The rheobase of the clothoidal electrode in D-5 at Time 0 is well above the rheobase of the conventional electrode, but at Time 8 the clothoidal rheobase is well below the conventional one. The limit threshold charge shows a similar behaviour. This was a common finding in our experiments, as will be reported elsewhere. In D-4 and D-5, relative to their values at implant, chronaxies of both, clothoidal and conventional electrodes, first decrease and then increase.

(D) Conclusions

(a) For a concave electrode a region located at a certain distance from electrode's surface is formed, where current density is higher and current lines are relatively parallel (**critical region of the electrode**).

(b) This critical region is both, farther away (from electrode's surface) and bigger, for clothoidal electrodes in comparison with other electrodes of the same size and material.

(c) At implant, the strength-duration curve for the conventional electrode was in general under the strength-duration curve for the clothoidal electrode. But after several days the situation suffered an inversion, mainly because conventional rheobases began to grow significantly meanwhile clothoidal rheobases didn´t grew so much, maintained its acute values **or even decreased**.

(d) In general, the clothoidal electrode showed a better sensing performance relative to the conventional electrode implanted in the same dog heart.

Bibliography

1. Aubert, A. and H. Hector (Editors) "*Pacemakers leads*", Elsevier, Amsterdam, 1985.
2. Baden-Fuller, A. "*Engineering field theory*", Pergamon Press, Oxford, 1973.
3. Fiandra, O. Suárez Antola, R. and others, "Endocardic stimulation. Observations after the implant of permanent leads", *Estimulación Cardíaca*, **2** (4), 209, 1981.
4. Fiandra, O. and others, "*Cardiac Pacemakers*", Department of Cardiology (School of Medicine, UdelaR) and National Institute of Cardiac Surgery, Montevideo, 1985 a.
5. Fiandra O. and others, "The cathode in cardiac stimulation: influence of its shape in chronic thresholds", *Annals of the VII Uruguayan Congress of Cardiology*, Montevideo, 1985 b.
6. Fiandra O. and R. Suárez-Antola, "*Electrode for electric stimulation of living tissues*", *UY*- Patent *12.817*, Montevideo, 1987.
7. Irnich, W. "The chronaxie time and its practical importance", *PACE*, **3**, 292, 1980.
8. Laplantif, J. "*Importance de la geometrie des electrodes dans la valeur du seuil aigu de stimulation cardiaque*", Ph. D. Thesis, Poitiers, 1983.
9. Ray, Ch. (Editor) "*Medical Engineering*", Year Book, Chicago, 1974.
10. Schaldach, M. y S. Furman (Editors), "Advances in pacemaker technology", Engineering in Medicine 1, Springer, Berlin, 1975.
11. Suárez-Ántola, R. "*Bio-mathematical perspectives of chronic cardiac pacing*", DPE, UdelaR, Montevideo, 1983.
12. Suárez-Ántola, R. "*Thresholds: Contributions to the study of excitation and propagation of the electric activity of biological tissues stimulated by external electrodes*", D.Sc. Thesis, PEDECIBA, UdelaR, Montevideo, 1994 a.
13. Suárez-Antola, R. "Concave Electrodes II: Theoretical Foundations", *Physics in Medicine and Biology*, **39 a**, 1994b.

14. Suárez-Antola, R. and G. Artucio, "Concave Electrodes III: Computer Assisted Design", *Physics in Medicine and Biology*, **39 a**, 1994.
15. Walton, C. Gergely, S. and A. Economides, "Platinum pacemakers electrodes: origins and effects of the electrode-tissue interface impedance", *PACE*, **10**, 87, 1987.

Physics in Medicine and Biology, vol. 39 a, 1994

CONCAVE ELECTRODES II: THEORETICAL FOUNDATIONS

Roberto Suárez-Antola

Dirección Nacional de Tecnología Nuclear, Ministerio de Industria, Energía y Minería, Montevideo, Uruguay

Introduction The geometry of the electrical current field generated by a given electrode in the volume conductor formed by biological tissues and the properties and position of the target region in excitable tissues, both determine the performance of the electrode as a stimulating and as a sensing device. Both from experimental facts and from theoretical reasons, the geometry of the current field of certain concave electrodes deserves special attention.

Materials and Methods For a field with a symmetry axis the distribution of current sources at electrode's surface is substituted by multipolar coefficients assigned to the electric centre of the electrode. Using Levenberg-Marquardt algorithm, the multipolar coefficients can be determined from suitable experimental results. Besides this, the current densities at any two points over the same field line are related by a functional of the mean curvatures of the points of the equipotential surfaces crossed by said field line between these two points. Then, Prim's theorem for solenoidal and almost gradient fields can be applied to the analysis of the **critical region of the electrode**, experimentally found as described in the first part of this work.

Results and Conclusions At points not too far away from the symmetry axis, the field can be well represented by three or four terms of the multipolar expansion, even in the case of concave electrodes. The electric potential, considered as a function of distance **on the symmetry axis**, shows an inflection point for concave electrodes and none for convex electrodes. This inflection point is the centre of the critical region of the electrode. The critical region of the electrode can be defined as a certain neighbourhood of the surface formed by the points where the equipotential surfaces have zero mean curvature. Its position and extension is the related with the multipolar coefficients of the field.

Key words: concave electrodes, clothoidal electrode, multipolar expansion of a potential field, solenoidal fields, almost gradient fields, critical regions, mean curvature, Prim's theorem.

Physics in Medicine and Biology, vol. 39 a, 1994

EXTENDED SUMMARY

(A) Introduction

The geometry of the electrical current field generated by a given electrode in the volume conductor formed by biological tissues and the properties and position of the target region in excitable tissues, both determine the performance of the electrode as a stimulating and as a sensing device. Both from experimental facts and from theoretical reasons, the geometry of the current field of certain concave electrodes deserves special attention.

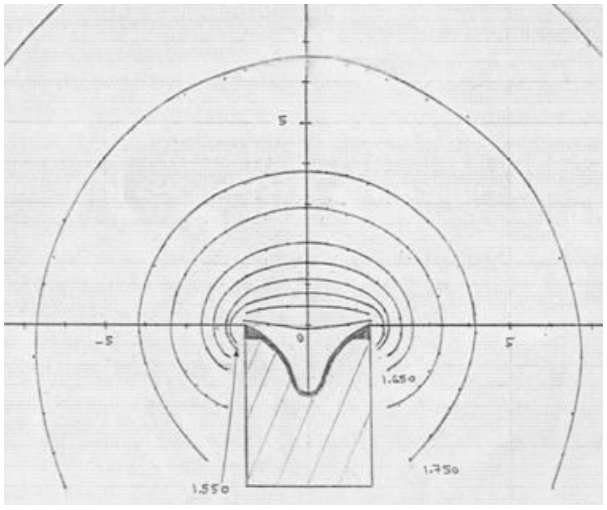

Figure 1. Sketch of the equipotential curves, clothoidal concave electrode

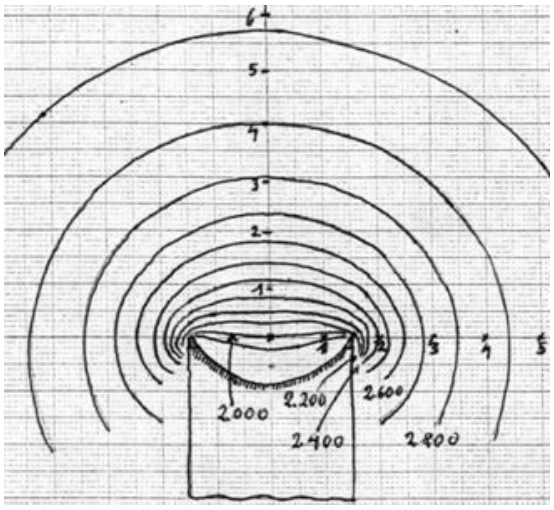

Figure 2. Sketch of the equipotential curves, hemispherical concave electrode

(B) Materials and Methods

(B. 1) Figure 3 shows a sketch of an electrode with an axis of rotational symmetry.

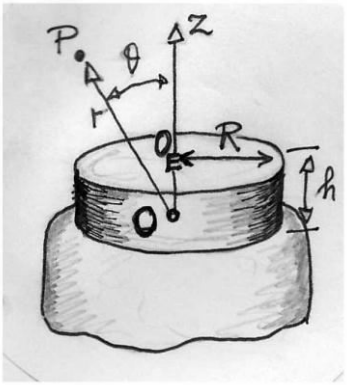

Figure 3. Sketch of an electrode's head with a set of polar coordinates r and θ on each symmetry plane through the axis z.

The distribution of current sources at electrode's surface can be substituted by a set of multipolar coefficients assigned to the electric centre of the electrode. Then for an unbounded, isotropic and homogeneous volume conductor, the electric potential $V(r,\theta)$ can be developed in terms of Legendre's polynomials and reciprocal powers of the polar distance r **, being** c_n **the** 2^n **multipolar coefficient** (Kellog, 1929):

$$V(r,\theta) = \sum_{n=0}^{n=+\infty} \frac{c_n}{r^{n+1}} \cdot P_n(\cos\theta) \qquad (1)$$

When the volume conductor is bounded but the symmetry of revolution is retained, it is necessary to add a constant term d_0 and terms involving increasing powers of r .

The origin of coordinates 0 (see Figure 3), when the electrode injects a net current in the volume conductor, can always be chosen to coincide with the so called electric centre, so that the coefficient of the dipolar term $c_1 = 0$. Taking this into account, we found that it is possible to approximate the equipotential surfaces measured in the upper region of the electrolytic tank, with focus in a neighbourhood of the z axis, by a formula that includes only a constant, a monopolar, a dipolar and an octupolar terms:

$$V(r,\theta) \approx d_0 + \frac{c_0}{r} + \frac{c_2}{r^3} \cdot P_2(\cos\theta) + \frac{c_3}{r^4} \cdot P_3(\cos\theta) \qquad (2)$$

The unknown multipolar parameters as well as the position of the electric centre in the symmetry axis can be estimated minimizing the following chi-squared variable, where $V(r_k,\theta_k)$ represents a measured voltage value at point (r_k,θ_k) in a vertical plane through the symmetry axis:

$$\chi^2(d_0,c_0,c_2,c_3) = \sum_{k=1}^{N} \left(V(r_k,\theta_k) - d_0 - \frac{c_0}{r_k} - \frac{c_2}{r_k^3} \cdot P_2(\cos\theta_k) - \frac{c_3}{r_k^4} \cdot P_3(\cos\theta_k) \right)^2 \qquad (3)$$

In this case $k = 1,2,...,N$ represents the points where the measurements were done.
The distance r_k between the electric centre of the electrode and the point where the voltage is measured is given by:

$$r_k^2 = r_0^2 + \rho_k^2 + 2 \cdot r_0 \cdot \rho_k \cdot \cos\varphi_k \qquad (4)$$

In formula (4): (1) ρ_k is the distance between the point 0_E of intersection of the symmetry axis z with the surface of the electrode's head, as shown in Figure 3, and the point P_k where the voltage is determined; (2) φ_k is the angle between the segment $0_E P_k$ and the z axis; and r_0 is the distance between 0 and 0_E (see Figure 3). It and can be called **electric radius** of the electrode. While ρ_k and φ_k can be measured directly, (r_k,θ_k) must be determined after the electric radius has been estimated, so in practice we have to work with the operational coordinates (ρ_k,φ_k) .

To estimate the multipolar coefficients and the electric radius r_0 it is possible to apply the Levenberg-Marquardt algorithm (Marquardt, 1963; Press and others, 1992) in two steps. First a gross estimation is obtained working with the voltage values on the electrode axis only. In this case we put $\theta = 0$ and $r = z + r_0$, so the following formula is used to estimate the unknown parameters r_0, d_0, c_0, c_2, c_3 :

$$V(z) \approx d_0 + \frac{c_0}{z + r_0} + \frac{c_2}{(z + r_0)^3} + \frac{c_3}{(z + r_0)^4} \tag{5}$$

Then, this gross estimation is used as seed to obtain a more accurate estimation employing all the measured values of voltage, according to formulae (3) and (4).

If A_0 is the area of the conductive electrode's head, then to begin the nonlinear iterations r_0 can be equalled to $\sqrt{\frac{A_0}{2 \cdot \pi}}$ A seed for parameters d_0, c_0 c_2 and c_3 can be estimated sequentially (as done in compartment analysis) from the numerical values of $V(z)$ when the distance on the axis of symmetry, from the surface of the electrode, grows.

(B. 2) Let us consider now a so called **almost gradient field**, like the electric current density $\vec{J}$ in an ohmic but perhaps heterogeneous volume conductor of variable (from point to point) scalar conductivity G :

$$\vec{J} = -G \cdot \nabla V \tag{6}$$

If the vectorial field is **solenoidal**, by definition the divergence of the field vanishes:

$$\nabla \bullet \vec{J} = 0 \tag{7}$$

According to Prim's theorem (Prim, 1948; Suárez-Ántola, 1984) for **solenoidal** and **almost gradient** fields, two of the following three conditions imply the third one:

1- The orthogonal surfaces to the field have zero mean curvatures.

2-The field is solenoidal.

3- The magnitude of the field along a field line is constant.

Equation (7) can be applied to almost stationary fields, that is, in conditions of slow enough time variation to be able to work with static equations. This is the case commonly encountered while pacing the heart or during functional electric stimulation of nerve and muscle fibres (Fiandra and others, 1985 a, Chapter 8; Reilly and others, 1992).

However, the volume conductor formed by biological tissues is often anisotropic. This is particularly important in the case of ventricular myocardium (Zipes and Jalife, 1990, Chapter 20). Now the relation between the current density vector field and the gradient of electric potential field is given by the equation

$$\vec{J} = -\tilde{G} \cdot \nabla V \tag{11}$$

The electrical conductivity $\tilde{G}$ is a positive definite symmetrical tensor. The current density field is not exactly almost-gradient as previously assumed. The bidomain model of ventricular myocardium, that is now used to analyse threshold and action potential propagation, takes into account the so called unequal anisotropy (different anisotropy ratios in the intacellular domain in comparison with the extracellular domain) and has important practical consequences (Suárez-Ántola, 1994 a)

(C) Results

(C.1) Figures 4 and 5 show the adjusting of formula (2) on the axis of symmetry of both, the plane and the clothoidal concave electrode (arrow 1,37cm), respectively, minimizing the

corresponding chi-squared by Levenberg-Marquardt algorithm. Formula (5) was employed with c_3 fixed at zero.

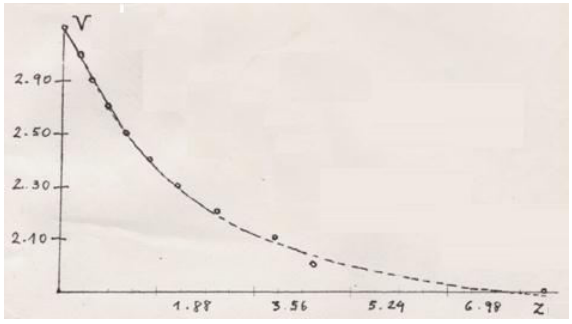

Figure 4

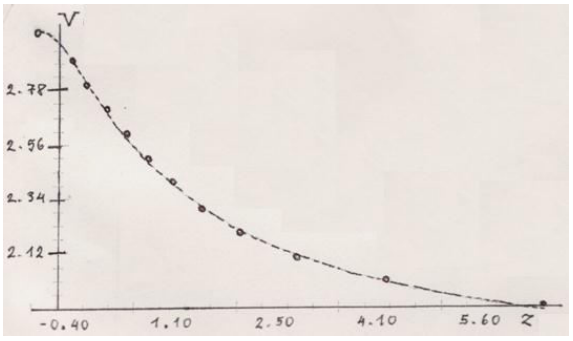

Figure 5

We found:

Plane electrode: $r_0 = 1.05\,cm \quad d_0 = 1.66V \quad c_0 = 2.13V \times cm \quad c_2 = -0.92V \times cm^3$

Clothoidal concave: $r_0 = 0.87\,cm \quad d_0 = 0.84V \quad c_0 = 1.01V \times cm \quad c_2 = -4.76\,V \times cm^3$

Since the multipolar coefficients c_n are proportional to the injected current, a more meaningful set of parameters is given by $\beta_n = \frac{c_n}{c_0}$.

For the clothoidal electrode with arrow 1,70cm, we found, including now the octupolar coefficient β_3 (and with a $\chi^2 = 1{,}88 \times 10^{-4}$):

$$\beta_2 = \frac{c_2}{c_0} = -0.466\ cm^2 \qquad \beta_3 = \frac{c_3}{c_0} = 0.089\ cm^3$$

For a clothoidal electrode with arrow 1,37cm, we found adjusting parameters with the complete set of measured voltages, including also the octupolar coefficient β_3:

$$\beta_2 = \frac{c_2}{c_0} = -0.65\ cm^2 \qquad \beta_3 = \frac{c_3}{c_0} = 0.25\ cm^3$$

A complete report of the estimation of parameters will be given elsewhere.

(C.2) Now, consider the mean curvatures of the equipotential surfaces near the axis of symmetry of a concave electrode in an isotropic and ohmic volume conductor. Near the concave surface of the electrode, mean curvatures are positive. But if we move along the axis away from the surface of the electrode, the mean curvature decreases until it vanishes at a certain point on the symmetry axis. In this point the curve that represents the voltage as a function of the abscissa z has an inflection point. This can be seen in figures 4 and 5.

In the case of a clothoidal electrode this inflection point is fairly distant from the electrode. In the case of a plane electrode, the inflection point doesn't exist.

Now, it is possible to apply Prim's theorem to a concave electrode taking into due account the continuity properties of the current field. We see that in the neighbourhood of the surface with zero mean curvature, the field lines will be almost parallel, the magnitude of the current density will be nearly constant along the field line and the magnitude of the

current density will be higher than its magnitude in points of the same field line away from the surface with zero mean curvature.

As consequence, a **critical region** is formed near the axis of a concave electrode, where the field lines are nearly parallel and more densely distributed.

(D) Conclusions

At points not too far away from the symmetry axis, the field can be well represented by three or four terms of the multipolar expansion, even in the case of concave electrodes.

The electric potential, considered as a function of distance on the symmetry axis, shows an inflection point for concave electrodes and none for convex electrodes.

This inflection point is the centre of the critical region of the electrode.

The critical region of the electrode can be defined as a certain neighbourhood of the surface formed by the points where the equipotential surfaces have zero mean curvature. Its position and extension is the related with the multipolar coefficients of the field.

Figure 6 shows a qualitative picture of the aforementioned critical region. In the last article of this series (Suárez-Ántola and Artucio, 1994) the position, size and shape of the critical region will be studied quantitatively.

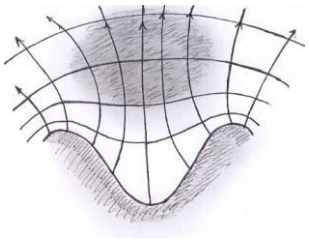

Figure 6

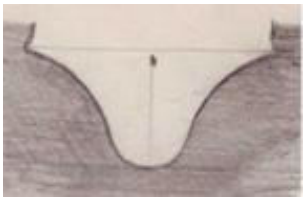

Figure 7

Figure 8

Figure 7 and 8 shows a template that was used to construct an optimum concave electrode and a photograph of the clothoidal electrode hand crafted by Dr. O. Fiandra using his jewelry's lather.

Bibliography

1. Brand, L. "*Vector and tensor analysis*", Wiley, New York, 1948.
2. Ericksen, J. "*Tensor Fields*", Appendix to Truesdall, C. and R. Toupin, "*The classical field theories*", Encyclopaedia of Physics, vol. III, Springer, Berlin, 1960.
3. Fiandra, O. and others, "*Cardiac Pacemakers*", Department of Cardiology (School of Medicine, UdelaR) and National Institute of Cardiac Surgery, Montevideo, 1985 a.
4. Fiandra O. and others, "The cathode in cardiac stimulation: influence of its shape in chronic thresholds", *VII Uruguayan Congress of Cardiology*, Montevideo, 1985 b.
5. Kellog, O. "*Foundations of potential theory*", Springer, Berlin, 1929.
6. Kline, M. and I. Kay, "*Electromagnetic theory and geometrical optics*", Interscience, New York, 1964.

7. Lindemans, F. "*Electrical stimulation of heart muscle*", Ph.D. Thesis, Elinkwijk, Uthretch, 1977.
8. Marquardt, D. "An algorithm for least-squares estimation of nonlinear parameters", *Journal of the Society for Industrial and Applied Mathematics*, **2**, 431, 1963.
9. Press, W. Flannery, B. Teukolsky, S. and W. Vetterling "*Numerical Recipes in C*", Cambridge University Press, Cambridge, 1992.
10. Prim, R. "On doubly laminar flow fields having a constant velocity magnitude along each sream-line", *U.S. Naval Ordnance Laboratory* Memoir Nº 9762, 1948.
11. Reilly, J. and others, "*Electric stimulation and electro-pathology*", Cambridge University Press, New York, 1992.
12. Suárez-Ántola, R. "Constant field electrode and chronic pacing of the heart", *II International Congress on Bio-mathematics*, Buenos Aires, 1984.
13. Suárez-Ántola, R. "*Thresholds: Contributions to the study of excitation and propagation of the electric activity of biological tissues stimulated by external electrodes*", D.Sc. Thesis, PEDECIBA, UdelaR, Montevideo, 1994 a.
14. Suárez-Ántola, R. Griego, J. and O. Fiandra, "Concave Electrodes I: Experimental Foundations". *Physics in Medicine and Biology*, **39 a**, 1994.
15. Suárez Antola, R. and G. Artucio, "Concave Electrodes III: Computer Assisted Design", *Physics in Medicine and Biology*, **39 a**, 1994.
16. D. Zipes y J. Jalife (Editors), "Cardiac electrophysiology: from cell to bedside", Saunders, Philadelphia, 1990.

Physics in Medicine and Biology, vol. 39 a, 1994

CONCAVE ELECTRODES III: COMPUTER ASSISTED DESIGN

Roberto Suárez Antola and Gabriel Artucio

Dirección Nacional de Tecnología Nuclear, Ministerio de Industria, Energía y Minería, Montevideo, Uruguay

Introduction The design of concave electrodes able to generate a critical region (C.R.) where current density is higher and field lines are relatively parallel, located at a certain distance from electrode's surface may be of interest both for electrical simulation of living tissues and for sensing tissue's own electrical activity (1). We present here a draft of a new design method that allows a sequential determination of size and shape of electrode's head, such that the electrode will be able to generate a C.R. of pre-established position and shape in given volume conductor, assuming an axis of symmetry for the desired field.

Materials and Methods The connection between geometric parameter of electrode's head and its C.R. is established trough the multipolar coefficients of the electric potential field (2). In a first stage we obtain an approximation to the monopole, quadrupole and octupole coefficients as functions of geometric parameter of C.R. (This relation is obtained from Whittaker's classical solution of Laplace's equation). In a second stage we simulate the potential field by means of a finite analytical approximation and make comparison of obtained C.R. with the desired one. If necessary we add some multipoles and proceed to a new digital simulation, and so on until we reach the desired degree of accuracy.

Results and Conclusions Then, we identify the point on the axis of symmetry of the field, where the potential has its extreme value before going into monotone variation towards zero. The equipotential surface that crosses the axis in this point can be adopted as the best model for size and shape of electrode's head. The proposed method doesn't involve the use of ab-initio numerical algorithms for the solution of the exterior boundary value problem of potential theory.

Key words: concave electrodes, clothoidal electrode, size and shape of the critical region, Whittaker's solution of Laplace equation, multipole expansions.

Physics in Medicine and Biology, vol. 39 a, 1994

EXTENDED SUMMARY

(A) Introduction

The shape and size of electrode's head have a strong influence both on acute and chronic pacing threshold and on the sensing performance of the electrode, when the target region is close enough to the surface of the electrode (Suárez-Antola, Griego y Fiandra, 1994).

The influence of the size and shape of the head of the electrode is due to the geometry of the electric current field generated by the electrode in the volume conductor formed by the biological tissues, and to the position of the target region (when pacing) or of the signal source (when sensing) in this volume conductor.

When the volume conductor can be considered as approximately homogeneous, isotropic and unbounded, the axisymmetric field of electric potential generated by a given symmetric electrode can be considered as produced by a certain set of multipolar moments. If the multipolar are located at the so-called electric centre of the current distribution the dipolar moment is always zero. At points not too far away from the symmetry axis, the field can be well represented by three or four terms of the aforementioned multipolar expansion: monopole, quadrupole, octupole and so on (Suárez-Antola, 1994).

This is so even in the case of concave electrodes. In concave electrodes a certain critical region, where current density is higher and field lines are relatively parallel, is produced at a certain distance from electrode's surface (Suárez-Antola, Griego y Fiandra, 1994; Suárez-Antola, 1994). We present here a sequential method to design a concave electrode's head such that it will be able to generate a critical region of pre-established position and shape in a given homogeneous and isotropic volume conductor, assuming an axis of symmetry for the desired potential field.

(B) Materials and Methods

Let us begin with Whittaker's solution (Copson, 1975) for Laplace's equation in cylindrical coordinates, written for a field with the axis z as its symmetry axis:

$$V(r,z) = \frac{1}{2\pi} \int_0^{2\pi} f(z + i \cdot r \cdot \cos\theta) \cdot d\theta \qquad [1]$$

Here r is the distance between the considered point and the axis. When r=0 (that is, on the axis z), V(0,z)=f(z), so that given the electric potential over the axis of symmetry its value at any other point can be found by formula [1].

Then we develop V(r,z) in powers of r up to order four at least (the coefficients of odd powers vanishes), first by approximating f(z+ircosθ) by a Taylor polynomial in ircosθ and then by calculating the error from Whittaker's formula.

The next stage is to introduce the multipolar expansion along z axis: $f(z) = \frac{I}{4\pi G} \sum_{n=0}^{\infty} \frac{\beta_{nn}}{z^{n+1}}$ where I is the total electric current, G is the electric conductivity of the tissues and the β_n are the multipolar coefficients, being $\beta_0 = 1$. If the origin z=0 is at the electric centere, then the dipolar coefficient $\beta_1 = 0$ and after the monopolar term we have to consider the quadrupole β_3, the octupole β_4 and so on.

In order to generate a critical region as was mentioned in the introduction, β_3 must be negative. Then, at a certain distance from z=0, along the z axis, f(z) (for I positive) reaches a maximum value for a certain $z=z_M$ and then tends monotonically towards zero while z grows. For $z=z_c$, f(z) shows an inflection point (that is $\frac{\partial^2}{\partial z^2} f(z_c) = 0$). The point (r=0, $z=z_c$) is going to be the centre of the intended critical region. We then consider $E_z = -\frac{\partial}{\partial z} V(r,z)$ and $E_r = -\frac{\partial}{\partial r} V(r,z)$. When r=0, E_r is always zero. $E_c = |E_z(0,z)|$ is maximum for z = zc.

Then we consider the region whose points (r,z) are such that $1 - \varepsilon \le \frac{|E_z|}{E_c} \le 1 + \varepsilon$ and $\frac{|E_r|}{E_c} \le \varepsilon$ for a given ε suitable chosen (for example ε=0.1).

Using a polynomial approximation for V(r,z) with a finite multipolar expansion for f(z), we can determine the size and shape of the critical region as a function of the field parameters. Conversely, given the dimension of the intended critical region, it is possible to estimate the corresponding field parameters. The size and shape of the surface of the electrode that generates such a critical region can be determined constructing the equi-potential surface that passes through the point $z=z_M$ of the axis of the field. If the result thus obtained is not good enough, another multipolar coefficient can be taken into account and the whole procedure must be repeated again.

(C) Results and Conclusions

The equipotential surface that crosses the point of the axis after which the fields decreases monotonically can be adopted as the best model for the size and shape of electrode's head.

The proposed method doesn't invoke the use of ab-initio numerical algorithms for the solution of the exterior boundary value problem of potential theory.

Instead, it only invokes the solution of fairly simple and well conditioned nonlinear algebraic equations (Press and others, 1992). After a certain size and shape for the electrode's head is selected, a detailed numerical study of the field can be done by more conventional means, or a sound physical scale model can be constructed and the potential field can be measured.

Bibliography

1. Copson, C. "Partial Differential Equations", Cambridge University Press, Cambridge, 1975.
2. Press, W., Flannery, B., Teukolsky, S. and W. Vetterling "Numerical Recipes in C", Cambridge University Press, Cambridge, 1992.
3. Suárez Antola, R. Griego, J. and O. Fiandra, "Concave Electrodes I: Experimental Foundations", *Physics in Medicine and Biology*, **39 a**, 1994.
4. Suárez Antola, R. "Concave Electrodes II Theoretical Foundations", *Physics in Medicine and Biology*, **39 a**, 1994.

Revista Iberoamericana de Sensores, 2006, vol. 5, Nº 2. ISSN 9974-0337.

Sensing bioelectric signals with concave electrodes: I. Lead Fields and Sensitivity

Roberto Suárez-Ántola
Departamento de Ingeniería Eléctrica, Facultad de Ingeniería y Tecnologías
Universidad Católica del Uruguay e-mail: rsuarez@ucu.edu.uy

Abstract

The shape and size of electrode's head may have a strong influence on the sensing performance, both of intra-cavitary electrodes and intra-tissue electrodes, whenever the sensed region is close enough to electrode's surface. The purpose of this paper is to discuss the performance of concave electrodes when used as sensing devices. The shape and size of a critical region of higher sensing sensitivity to the electric activity of biological tissues is studied using a mathematical model of a homogeneous and isotropic volume conductor. A formula is derived for the measured potential difference between a proximal concave electrode and a distal indifferent one, due to tissues' electrical activity.

Keywords: bioelectric sensors, bioelectric signals, concave electrodes.

(A) Introduction:

Sensors of bioelectric phenomena are usually known as electrodes. As every other biomedical sensor, they serve as interfaces between biological tissues and electronic equipment for diagnostic or research purposes. Both biologic and electronic parameters have influence on the sensing performance of the electrode, so that they must be considered during electrode's design. Sensing electrodes are designed to fulfil with three conditions: (1) Provide an output signal proportional to the measured bioelectric quantity. (2) To be insensitive to other physical quantities. (3) Minimize the unavoidable effects due to bioelectric activities of other origin and noises of several kinds. Intracavitary and intratissue electrodes are often used both for diagnosis and therapy, so that the two kinds of application must be considered during electrode's design.

This is the case of intracavitary electrodes used to take cardiac electrograms and to pace the heart. This is done with the same electrode located at the tip of a catheter that is introduced (following a venous path) in the right cardiac cavities. Once the electrode is implanted, the presence of foreign materials produces an inflammatory reaction followed by the formation of a capsule of fibrous tissue that surrounds the electrode's head. Therefore, the local properties of the volume conductor change, so that the sensing and the stimulating properties of the electrode may change. This and many other problems must be considered in the process of design of heart electrodes, most of them with convex shapes but with geometric details that are introduced to improve their sensing and pacing performance [1].

During 1983 appeared the idea of pacing the heart with concave electrodes, instead of the then standard convex ones. Some prototypes of concave electrodes were developed in France [2] (parabolic-concave), in Uruguay [3] (clothoidal-concave), and later in other places.

Now, it is well known that both the shape and size of electrode's head have a strong influence on acute and chronic pacing threshold as well as on the sensing performance of the electrode if the target region (for stimulation or sensing) is close enough to electrode's surface. Although this influence is particularly relevant in the case of myocardium pacing [4], it could be of interest both for pacing [5] and sensing the local electrical activity of the nervous system, skeletal muscle, and smooth muscle. The sensing properties of concave electrodes have not been much studied, and even then, only experimentally and in a global approach [6], without considering the distribution of local sensitivities as given by the lead field of the sensing electrodes.

The lead field concept arises when two electrodes are placed in a volume conductor forming what is called a lead [7], [8].

The lead vector $\vec{u}(\vec{r})$ describes how an electromotive source of vector density $\vec{E}_S(t,\vec{r})$ (located at the point of position vector $\vec{r}$ and at the time instant t) influences the lead voltage V_L recorded between the electrodes, being $\vec{u}\cdot\vec{E}_S$ a scalar product:

$$V_L\ t\ = \int_B \vec{u}\ \vec{r}\ \cdot \vec{E}_S\ t,\vec{r}\ \ d\nu \qquad (1)$$

The integration is, in principle, extended to the whole tissue's ohmic volume conductor represented by the three-dimensional region B.

For a given lead vector, the contribution of a given vector density of electromotive force is proportional to the cosine of the angle between them. If $\vec{E}_S$ is orthogonal to $\vec{u}$ it will not contribute to the measured voltage signal, and the contribution will be maximum in absolute value if the two vectors are parallel. The contribution of a given local electromotive force density will be proportional to the magnitude of the local lead vector $\vec{u}(\vec{r})$. So, the local lead vector describes the sensitivity of the lead to a source located there. The distribution of the lead vectors in the volume conductor is the lead field, and this field gives the distribution of sensitivities of the system (the lead) formed by the volume conductor (biological tissues) and the electrodes. It follows from **the reciprocity principle** [8] that **the lead field $\vec{u}(\vec{r})$ is identical with the field of electric current density** that is produced in the volume conductor when **a unit current** (called the **reciprocal current**) is fed to the lead from the outside. The directions of the lead field flow lines give the directions of the sensitivity, and their density is proportional to the local magnitude of the sensitivity. This density is higher near each electrode, so that ceteris paribus (other things remaining the same) the electric signals produced in the neighbourhood of the electrode receive a higher weight in the determination of the output signal $V_L\ t$. For convex electrodes the sensitivity grows when the distance to the electrode decreases and reaches a maximum value at the interface between the electrode and the tissues. For example, in the case of a spherical electrode of radius r_0, immersed in an isotropic, homogeneous and ohmic volume conductor, the lead field is given by:

$$\vec{u}\ r,\phi,\theta\ = (\frac{1}{4\pi r^2})\vec{e}_r\ \ \phi,\theta \qquad (2)$$

Here r is the distance from the centre of the electrode, and φ,θ are the angular spherical coordinates of the unit vector $\vec{e}_r$ directed outwards. The magnitude of the lead field vectors is maximum on the surface of the electrode, where r reaches its minimum value r_0. (Equation (2) follows from the relation $4\pi r^2\ j\ r\ = I$ between the global current I injected through the electrode and the current density j, taking into account that the magnitude of the local lead vector is $u\ \vec{r}\ = \frac{j\ \vec{r}}{I}$ and due to the assumed spherical symmetry is directed radially outwards).

The purpose of this paper is to discuss some interesting properties of concave electrodes when used as sensing devices. This is done in the framework of the theorem of reciprocity for a heterogeneous and anisotropic conductive medium with a distribution of current sources (electromotive forces) in its interior and a pair of **sensing electrodes** on its boundary. One electrode is **active**, **concave**, and **located very close** to the **region of interest**, and the other **indifferent**, with a **much bigger surface**, and **far from this region**.

(B) The lead field for concave electrodes

Now we will show that for concave electrodes of a suitably selected shape there is a **critical region**, located at a certain distance from the surface of the electrode, where the density of lead field lines is higher than in any other region (including regions located nearer to electrode's concave surface) and the lines are relatively parallel (Fig. 1) .

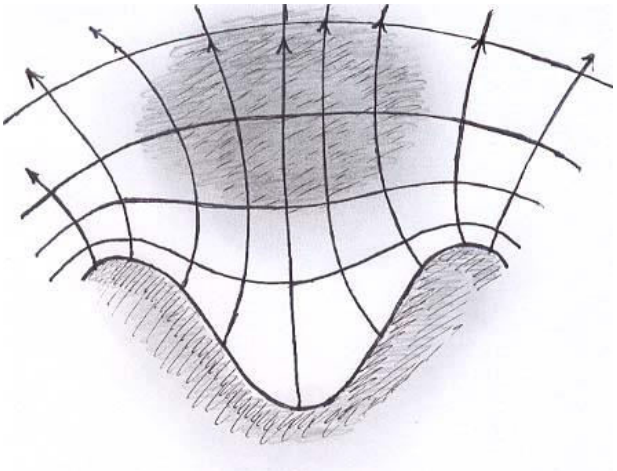

Fig.1: Pictorial representation of a meridian cross section of a concave electrode. Sketch of the lead field lines and of some equipotential surfaces. The critical region appears at some distance adjacent to the axis of symmetry of the lead field.

The shape and size of this critical region of higher sensing sensitivity to the electric activity of biological tissues may be studied using a mathematical model of a homogeneous and isotropic volume conductor, as functions of the size and shape of the surface of the electrode.

So, we consider a symmetric electrode immersed in an unbounded ohmic volume conductor, with the indifferent electrode located far away.

In this case the electric potential field inside the volume conductor verifies Laplace's equation. A convenient starting point in this case is Whittaker's solution for Laplace's equation [9], assuming cylindrical symmetry in the electric potential field V inside the volume conductor:

$$V(\rho,z) = \frac{1}{2\pi}\int_0^{2\pi} f(z + j\rho\cos\theta)\, d\theta \qquad (3)$$

Here ρ is the distance between the considered point and the z axis. When $\rho = 0$ (that is, on the z axis) $V(0,z) = f(z)$, so that given the electric potential over the axis of symmetry its value at any other point can be found by formula (3).

Then we develop $V(\rho,z)$ in powers of ρ up to order four at least (the coefficients of odd powers vanish), first by approximating $f(z + j\rho\cos\theta)$ by a Taylor polynomial in $j\rho\cos\theta$ and then by calculating the corresponding terms and the error $R(\rho,z)$ from Whittaker's integral formula:

$$V(\rho,z) = Z_0(z) + \rho^2 Z_2(z) + \rho^4 Z_4(z) + R(\rho,z) \qquad (4)$$

By definition:

$$Z_0(z) = f(z),\ Z_2(z) = -\frac{1}{4}\frac{d^2 Z_0(z)}{dz^2}$$

$$Z_4(z) = \frac{1}{64}\frac{d^4 Z_0(z)}{dz^4} \qquad (5)$$

Furthermore, the remainder: $R(\rho,z) = 0(\rho^6)$

The next stage is to introduce the multi-polar expansion of the electric potential along z axis:

$$Z_0(z) = f(z) = \frac{I}{4\pi G}\sum_{n=0}^{\infty}\frac{\beta_n}{z^{n+1}} \qquad (6)$$

In this formula I is the total injected electric current, G is the electric conductivity of the tissues and the parameters β_n are the so called **multi-polar coefficients**. $\beta_0 = 1$. In the case of a potential field with a nonzero mono-polar coefficient, the origin $z = 0$ can be suitably chosen at the electric centre of the distribution of field sources [10]. Then the dipolar coefficient $\beta_1 = 0$ and after the mono-polar term we must consider the quadrupole β_2, the octupole β_3 and so on. The following expansion for the potential $V(0,z)$ is enough for our purposes:

$$f(z) \approx \frac{I}{4\pi G}\left[\frac{1}{z} + \frac{\beta_2}{z^3} + \frac{\beta_3}{z^4}\right] \qquad (7)$$

The local lead vector sensitivity is calculated from its scalar components, $u_z = -\frac{\partial V}{\partial z}$ $u_\rho = -\frac{\partial V}{\partial \rho}$ for a unit global current $I = 1$, using the first multi-polar coefficients β_2 and β_3 as the only parameters.

$$u_z \approx -\left[\frac{df(z)}{dz} - \frac{\rho^2}{4}\frac{d^3 f(z)}{dz^3} + \frac{\rho^4}{64}\frac{d^5 f(z)}{dz^5}\right] \qquad (8a)$$

$$u_\rho \approx -\left[-\frac{\rho}{2}\frac{d^2 f(z)}{dz^2} + \frac{3\rho^3}{64}\frac{d^4 f(z)}{dz^4}\right] \qquad (8b)$$

The coefficients β_2 and β_3 can then be related with the size and shape of the sensing electrode's head. This can be done either measuring the distribution of the electric potential adjacent to the symmetry axis and estimating the parameters from the experimental data [6] or making a digital simulation of the potential field produced by the electrode. To generate a critical region as was mentioned in the introduction β_2 must be negative (Fig. 2).

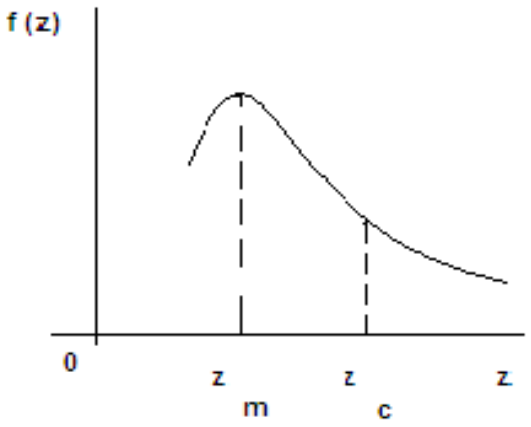

Fig.2: Pictorial qualitative sketch of the voltage on the axis of symmetry of the sensing concave electrode.

Then, at a certain distance from $z = 0$, along the z axis, $f(z)$, for I positive, (in the lead field's case equal to 1), reaches a maximum value for a certain $z = z_M$ and then tends monotonically towards zero while z grows. The function $f(z)$ has a negative slope for z greater than z_M. When z is near enough to z_M its second derivative is negative. However, for z positive and big enough, the function tends to zero with positive second derivative. Then, there is a certain $z = z_c$ such that $f(z)$ shows an inflection point: $\frac{d^2}{dz^2} f(z_c) = 0$

The point $\rho = 0, z = z_c$ is going to be the centre of the intended critical region. We then consider the scalar components of the lead vector, according to

formulae (8a) and (8b). When $\rho = 0$, then the radial component u_ρ is always zero. The absolute value of the axial component $u_{axis}(z) = |u_z(0,z)|$ takes its maximum for $z = z_c$.

Now we have:

$$f(z) \approx f(z_c) + \frac{df(z_c)}{dz}(z - z_c) + \frac{1}{6}\frac{d^3 f(z_c)}{dz^3}(z - z_c)^3$$

Let us consider the length scale: $l_c^{\,2} = \dfrac{\left|\dfrac{df(z_c)}{dz}\right|}{\left|\dfrac{d^3 f(z_c)}{dz^3}\right|}$ (9)

This scale characterizes the length along the z axis in which the component of the lead field u_z, suffers a significant variation.

Then, we define the dimensionless space coordinates:

$$\xi = \frac{\rho}{l_c} \quad (10a) \qquad \eta = \frac{z - z_c}{l_c} \quad (10b)$$

From equations (8a) and (8b), and from the definitions (10a) and (10b), it follows that the components of the lead field near the point: $\rho = 0$ $z = z_c$ can be expressed as:

$$\frac{u_\rho}{u_c} \approx s\left(\frac{\xi\eta}{2}\right) \qquad (11a)$$

$$\frac{u_z}{u_c} \approx 1 + s\left(\frac{\xi^2}{4} - \frac{\eta^2}{2}\right) \qquad (11b)$$

Here, by definition, $s = sign\left[\dfrac{d^3 f(z_c)}{dz^3}\right]$

It is equal to 1 in our case. Then we consider a region extending symmetrically around the z axis, and centred in $z = z_c$ whose points ρ, z are such that $1 - \varepsilon \le \dfrac{|u_z|}{u_c} \le 1 + \varepsilon$ and $\dfrac{|u_\rho|}{u_c} \le \varepsilon$ for a given ε suitable chosen (for example $\varepsilon = 0.1$). This region is a critical region of the leading field in the sense mentioned at the beginning of this section (B). The sensitivity lines are almost parallel and their density there is greater than in other regions of the lead field. This is so because the magnitudes of the local lead vectors are very near their possible maximum value u_c in any region adjacent to the z axis.

(C) The lead voltage: a general formula

Concave electrodes show variable curvatures, in magnitude and in sign, from point to point on their surfaces. The concavity is surrounded by a convex ring. The current density is smaller in the points located on the concavity than in the points located in the convex portions [11]. As consequence, the degree of polarization of the interface is greater in the convex part than in the concave one, so that the voltage drop will be different at different points of the electrode's surface. The influence of the voltage drop in the electrochemical double layer located at the interface between the concave electrode and the tissues, for a polarizing concave electrode, may be taken into account by means of the introduction of a family of virtual non-polarizing concave electrodes of smoothly varying shapes. In each instant, one electrode belonging to the family represents the local time behaviour of the polarizing electrode. The voltage drop at the indifferent electrode is assumed negligible due to its big area. The geometry of the equivalent volume conductor is identical with the real one, except in the vicinity of the already mentioned family of non-polarizing concave electrodes.

Let us sketch the derivation of a new formula that generalizes formula (1) to this more complex situation.

We represent by $\hat{G}$ the conductivity tensor of the tissues, and by $\vec{J} = -\hat{G}\cdot\nabla V + \hat{G}\cdot\vec{E}_S$ the current density produced by the combined effect of a potential gradient and a local electromotive force. This is the current field produced in the volume conductor by the electrical activity of the tissues.

Under quasi-stationary conditions, the density current field generated by the tissues verifies:

$$\nabla\cdot\vec{J} = 0$$

The conductivity tensor is symmetric, so that $\vec{a}\cdot\hat{G} = \hat{G}\cdot\vec{a}$ for any vector $\vec{a}$.

In the boundary of the volume conductor there aren't electromotive forces and with the only exception of the points that belong to the surfaces of the electrodes, the boundary condition is $\vec{J}\cdot\vec{n} = 0$.

On the electrode surfaces the quasi-stationary electric potentials can be taken as constants and equal to V_1 and to V_2 respectively, so that the lead voltage is given by: $V_L = V_1 - V_2$

When the current is injected through the lead from outside, the current density will be represented by $\vec{j} = -\hat{G}\cdot\nabla\varphi$, being ϕ the induced electric

potential in the tissues due to the external current only.

We also have $\nabla \cdot \vec{j} = 0$ and the same boundary conditions for ϕ as given before for V.

Now, we consider stationary alternating currents of frequency: $\omega = 2\pi f$

The phasor amplitudes of the scalars potentials $\dot{\varphi}\ \omega, \vec{r}$, $\dot{V}\ \omega, \vec{r}$ and the phasor amplitudes of the vector fields $\dot{\vec{J}}\ \omega, \vec{r}$, $\dot{\vec{j}}\ \omega, \vec{r}$ verify the following equations:

$$\nabla \dot{\varphi} \cdot \dot{\vec{J}} = \nabla \dot{V} \cdot \dot{\vec{j}} - \dot{\vec{j}} \cdot \dot{\vec{E}}_S \qquad (12)$$

From vector analysis tools it follows:

$$\int_B \nabla \dot{V} \cdot \dot{\vec{j}}\, d\nu = \int_B \nabla \cdot \dot{V}\, \dot{\vec{j}}\ d\nu - \int_B \dot{V}\ \nabla \cdot \dot{\vec{j}}\ d\nu$$

Considering that $\nabla \cdot \dot{\vec{j}} = 0$ we obtain:

$$\int_B \nabla \cdot \dot{V}\, \dot{\vec{j}}\ d\nu = \int_{\partial B} \dot{V}\ \vec{n} \cdot \dot{\vec{j}}\ d\nu = \dot{V}_L\, \dot{I} \qquad (13\ a)$$

Here $\dot{I} = \int_{\partial B_e} \dot{\vec{j}} \cdot \vec{n}\, dS$ is the phasor amplitude of current introduced through the electrodes into the tissues volume conductor.

Also, we have:

$$\int_B \nabla \dot{\phi} \cdot \dot{\vec{J}}\ d\nu = \int_B \nabla \cdot \dot{\phi}\, \dot{\vec{J}}\ d\nu - \int_B \dot{\phi}\ \nabla \cdot \dot{\vec{J}}\ d\nu$$

Considering that $\nabla \cdot \dot{\vec{J}} = 0$ we obtain:

$$\int_B \nabla \cdot \dot{\phi}\, \dot{\vec{J}}\ d\nu = \int_{\partial B} \dot{\phi}\ \vec{n} \cdot \dot{\vec{J}}\ d\nu = \dot{\phi}_1 - \dot{\phi}_2\ \dot{I}' \qquad (13\ b)$$

$\dot{I}'$ is the phasor amplitude of the global current produced by the electromotive forces associated with the electric activity of the biological tissues.

From all these relations we derive

$$\int_B \nabla \dot{\varphi} \cdot \dot{\vec{J}}\, d\nu = \dot{\varphi}_1 - \dot{\varphi}_2\ \dot{I}' = \dot{V}_L\ \dot{I} - \int_B \dot{\vec{j}} \cdot \dot{\vec{E}}_S\, d\nu \qquad (14)$$

Then, if $\dot{Z}_{ext}\ \omega$ is the impedance due to the external measuring circuit between the electrodes,

$$\dot{V}_L\ \omega = \dot{Z}_{ext}\ \omega\ \dot{I}'\ \omega \qquad (15)$$

If $\dot{Z}_T\ \omega$ is the impedance due to the in-series combination of the ohmic resistance of the tissues R_T with the lumped impedance $\dot{Z}_e\ \omega$ of the polarizing interface between the electrode and the tissues, then:

$$\dot{\varphi}_2\ \omega - \dot{\varphi}_1\ \omega = \dot{Z}_T\ \omega\ \dot{I}\ \omega \qquad (16)$$

Introducing $\dot{\vec{u}} = \frac{1}{\dot{I}} \dot{\vec{j}}$ from equations (14), (15), and (16) it follows, after several calculations:

$$\dot{V}_L\ \omega = \frac{1}{\left(1 + \frac{\dot{Z}_T\ \omega}{\dot{Z}_{ext}\ \omega}\right)} \left(\int_B \dot{\vec{u}}\ \omega, \vec{r}\ \cdot \dot{\vec{E}}_S\ \omega, \vec{r}\ \ d\nu \right) \qquad (17)$$

This formula is a nontrivial generalization of equation (1). The phasor component $\dot{V}_L\ \omega$ of the voltage sensed by the lead that corresponds to the frequency ω , is expressed as a functional of the distribution of phasor vector electromotive forces, $\dot{\vec{E}}_S\ \omega, \vec{r}$, in the tissue's volume conductor, and the phasor lead's vector field $\dot{\vec{u}}\ \omega, \vec{r}$ produced in the volume conductor by an alternating unit current injected from outside through the sensing electrodes. The lead field $\dot{\vec{u}}\ \omega, \vec{r}$ may depend on the frequency due to the different degrees of polarization of the points on the surface of a concave electrode if the mean curvatures differ between these points.

(The impedance $\dot{Z}_e\ \omega$ may be given by the formula derived in [13]:

$$\dot{Z}_e\ \omega = \frac{R_d}{\left(1 + j \frac{\omega}{\omega_d}\right)^m}$$

Here m is a positive number, less than 1, related with the fractal dimension of the interface, R_d is a D.C. resistance of the polarized interface, and ω_d is a characteristic angular frequency that separates the constant phase angle behaviour of the interface at high frequencies from its resistive faradic behaviour at low frequencies).

If the impedance of the external circuit is at least an order of magnitude greater than the combined impedance of the tissues and interfaces, (17) simplifies into: $\dot{V}_L\ \omega\ = \int_B \dot{\vec{u}}\ \omega,\vec{r}\ \cdot \dot{\vec{E}}_S\ \omega,\vec{r}\ \ d\nu$

When the polarization of the interface does not modify significatively the lead field, $\dot{\vec{u}}\ \omega,\vec{r}\ \approx \vec{u}\ \vec{r}$

Then, returning to the time domain we obtain formula (1) given in the introduction.

(D) Discussion and conclusions

(a) The problem of determining the geometric parameters of an electrode's head such that it produces a critical region with suitable shape and size can be approximately solved by an analytical approach. Let us observe first that the electric conductivity of the electrode's material is at least several orders of magnitude greater than the conductivity of the tissues and the body fluids. As consequence, the surface of the electrode may be safely assumed to be a surface of equal potential of the electric potential field produced by the electrodes when the reciprocal current is injected to the lead from outside. In principle any surface $V(\rho,z)$=constant could be a candidate to a surface of a suitable electrode. However, this cannot be exactly this way if the surface of equal potential is unbounded. But if our interest is focussed into the abovementioned critical region located near the axis of symmetry, it is possible to construct a suitable approximation to the shape and size of the electrode to produce the desired field within established tolerance bounds. This will be studied in the second part of the present work. Nevertheless, the procedure can be briefly sketched for an unbounded, isotropic and homogeneous volume conductor.

Let us consider Whittaker's formula again. We introduce a function $z=g(\rho)$ such that:

$$V\ \rho,g\ \rho\ = \frac{1}{2\pi}\int_0^{2\pi} f\ \ g\ \ \rho\ + j\rho\cos\theta\ \ d\theta = V_0 \qquad (18)$$

The function $z=g(\rho)$ represents the trace of the surface of constant potential, V_0, in a plane that contains the axis of symmetry of the field. In principle, given V_0 and assuming enough regularity in the functions $f(z)$ and $g(\rho)$ we can calculate all the derivatives of $g(\rho)$ in $\rho=0$, from (18), as functions of the parameters β_2 and β_3

This can be done by successive derivation operations under the integral sign, relatives to ρ, and putting each result equal to zero.

An approximation of order four may thus be obtained:

$$z = g\ \ \rho\ \approx z_0 + \frac{1}{2}\frac{d^2 g\ \ 0}{dz^2}\rho^2 + \frac{1}{24}\frac{d^4 g\ \ 0}{dz^4}\rho^4 \qquad (19)$$

For a concave electrode of depth d and radius R_0, we may write:

$$z = g\ \ \rho\ \approx z_0 + \frac{2d}{R_0{}^2}\rho^2 - \frac{d}{R_0{}^4}\rho^4 \qquad (20)$$

The geometric parameters d and R_0 are determined from the derivatives of the function $g(\rho)$ on the axis of symmetry, and these derivatives are then related with the multi-polar coefficients of the field. The parameter z_0 must be chosen near but somewhat greater than the parameter z_M where the function $f(z)$ takes its maximum value, in order that the current density may have the same sign everywhere in the surface of the electrode.

Then $z_c - d$ will give the distance, along the symmetry axis, from the centre of the critical region to the electrode. See Fig. 3.

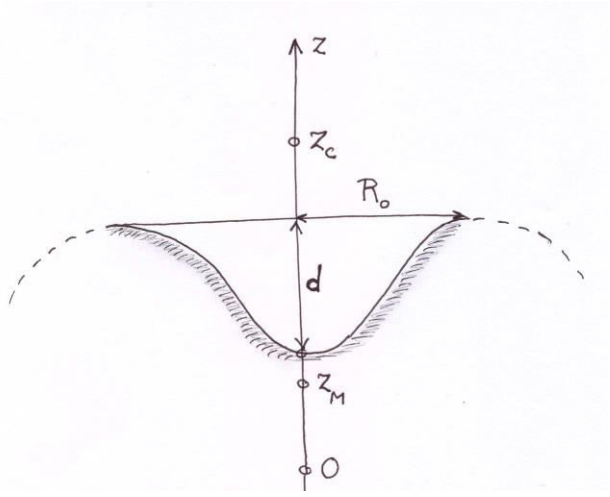

Fig.3: Qualitative sketch of the curve corresponding to formula (20). The depth d and the radius R_0 of the concave electrode appear, as well as z_M and the centre of the critical region z_c.

(b) The lead field adjacent to a polarizing concave electrode was studied from a mathematical viewpoint, and the resultant distribution of sensing sensitivities was given through approximate

analytical formulae for the scalar components of the lead field (8a) and (8b).

(c) The critical region for sensing with concave electrodes was defined and approximate analytical formulae for the scalar components of the lead field were obtained in (11a) and (11b).

(d) A generalization of formula (1), that relates the lead voltage $V_L(t)$ with the lead field $\vec{u}(\vec{r})$and the distribution of electromotive forces $\vec{E}_S\ t,\vec{r}$ in the volume conductor, was given, for alternating current signals, in formula (17). The amplitudes $\vec{u}(\omega,\vec{r})$ of the oscillating lead field may differ significantly from $\vec{u}(\vec{r})$ only near the concave electrode surface. Far from this surface the effects due to the curvatures vanish and the potential field resembles the field of a convex spherical electrode.

(e) The lead field was studied using a model of an isotropic and homogeneous volume conductor. In the cases of many tissues, and in the case of myocardium in particular, the volume conductor is anisotropic and heterogeneous, so the study should be extended to embrace this more general case.

(f) Every concave electrode has curved convex borders. The magnitude of the lead field (and as consequence the sensitivity to bio-electric signals) is higher there than in the critical region. Nevertheless, the fibrous capsule of connective tissue that surrounds the chronic pacing electrodes, in most cases extends over this region and beyond. So, this potentially higher sensitivity has no chance to manifest itself after a few weeks from the implantation.

(E) References

[1] G.Mond, "*Recent advances in pacemaker leads*", Cardiac Electrophysiol. Rev. vol 3, pp5-9, 1999.

[2] A. Amiel, J. Besson and G. Lehmann, "*The convergent field tip: A clinical comparison with regular leads*", in A.Aubert and H.Hector (Eds) "Pacemakers leads", Amsterdam: Elsevier, 1985.

[3] O.Fiandra and R.Suárez-Antola: "*Electrodo para estimulación eléctrica de tejidos vivos*", Memoria descriptiva de la patente uruguaya *Nº 12.817*, Montevideo, 1987.

[4] S.Furman, D.Hayes, and D.Holmes, "A practice of cardiac pacing", Futura, San Francisco, 1993.

[5] R.Suárez-Ántola, "*The time constants for the electric stimulation of nerve and muscle fibers by point electrodes*", Proceedings of the 2nd IEEE-EMBS International Conference on Neural Engineering, IEEE Press, pp 652-655, 2005.

[6] R.Suárez-Ántola, J.Griego and O.Fiandra: "*Concave electrodes I: Experimental foundations*", Physics in Medicine and Biology, vol.39a, pp 413-419, 1994.

[7] J.Malmivuo, "*Biomagnetism*", Chapter 16 in J.Bronzino (Ed.) "Biomedical Engineering Handbook", 3ª Ed, Boca-Raton: CRC, 2006.

[8] R.Arzbaecher and D.Brody, "*The lead field: vector and tensor properties*", Chapter 7 in C.Nelson and D.Geselowitz (Eds.), "The theoretical basis of electrocardiology", Clarendon Press, Oxford, 1976.

[9] E.Copson, "Partial Differential Equations", Chapter 11, Cambridge University Press, Cambridge, 1975.

[10] A.Kompaneyetz, "Theoretical Physics", p134, Peace publishers, Moscow, 1961.

[11] R. Suárez-Ántola, "*Chronic cardiac pacing: a bio-mathematical approach*", Chapter 8 in O.Fiandra (Ed.), "Cardiac Pacemakers", CCC, Montevideo, 1985 (in Spanish, although a translation to English of Chapter 8 was made under the request of S.Furman).

[12] A.Borisenko and I.Taparov, "Vector and Tensor Analysis",Dover, N.Y., 1979.

[13] R. Suárez-Ántola: "*Thresholds: Contributions to the study of excitation and propagation of the electric activity of biological tissues stimulated by external electrodes*", D.Sc. Thesis, Chapter 1, part E, PEDECIBA, UDELAR, Montevideo, 1994, (in Spanish).

Revista Iberoamericana de Sensores, 2008, vol. 6, Nº 1, pp. 114-121. ISSN 9974-0337.

Sensing bioelectric signals with concave electrodes:

II. Experimental and analytical approaches to electrode design

Roberto Suárez-Ántola
Departamento de Ingeniería Eléctrica, Facultad de Ingeniería y Tecnologías
Universidad Católica del Uruguay
11600 Montevideo, Uruguay
e-mail: robertosua@gmail.com

Abstract

As shown in the first part of this work, the shape and size of electrode's head may have a strong influence on the sensing performance, both of intra-cavitary electrodes and intra-tissue electrodes, whenever the sensed region is close enough to electrode's surface. The purpose of this second paper is threefold: (a) Review some experimental results obtained for the lead fields and the corresponding sensitivities of a set of metal electrodes of different shapes and suitably enlarged size to use an electrolytic tank and comparing these results with the mathematical model for concave electrodes immersed in homogeneous and isotropic volume conductors developed in the previous paper. (b) Derive in the time domain a formula for the measured potential difference between a **polarisable** proximal concave electrode and a distal indifferent one, due to tissues' electrical activity. (c) Give some guidelines to be applied in the conceptual design of concave electrode heads intended to sense bioelectric signals generated in electromotive sources imbedded in heterogeneous and anisotropic tissues. A virtual space (alibi), homogeneous and isotropic, is introduced in correspondence with physical space. The design problem is easier to pose and analyze in this auxiliary space. Then the results may be transformed back to the physical space.

Keywords: bioelectric sensors, bioelectric signals, concave electrodes, tissue's anisotropy, and heterogeneity.

Introduction:

Sensors used to detect and measure bioelectric phenomena are known as electrodes. They serve as interfaces between biological tissues and electronic equipment, for diagnostic, therapeutic or research purposes. Both biologic and electronic parameters have influence on the sensing performance of the electrode, so that they must be taken into account during electrode's design.

Sensing electrodes are designed to fulfil with three conditions:

(1) Provide an output signal proportional to the measured bioelectric quantity.

(2) To be insensitive to other physical quantities. (3) Minimize the unavoidable effects due to bioelectric activities of other origin and noises of several kinds.

As was shown in the first paper of this series [1], both the shape and size of electrode's head may have a strong influence on the sensing performance of an electrode. This occurs if the **target region for sensing** (that is the region where the distribution of electromotive forces of interest is located), is close enough to the surface of the sensor.

Although the shape of most electrode heads is convex, several years ago a generation of concave electrode heads was introduced, mainly but not exclusively, with the intention to improve electrode's performance during cardiac pacing [1], [2], [3]. To characterize the sensing properties of concave electrodes, it is necessary to study first the distribution of local sensitivities in the tissue's volume conductor as given by the **lead field** [4], [5] of the sensing electrodes. The (for the time being assumed stationary) lead vector $\vec{u}(\vec{r})$ describes how an electromotive source of vector density $\vec{E}_S(t,\vec{r})$, varying with time t and located at the point of position vector $\vec{r}$ influences the lead voltage $V_L(t)$ recorded between the electrodes:

$$V_L(t) = \int_B \vec{u}(\vec{r}) \cdot \vec{E}_S(t,\vec{r})\, d\nu \qquad (1)$$

The integration is, in principle, extended to the whole tissue's ohmic volume conductor represented by the three-dimensional region B ($\vec{u}.\vec{E}_S$ is a scalar product). For a given lead vector, the contribution of a given vector density of electromotive force is proportional to the cosine of the angle between them. If $\vec{E}_S$ is orthogonal to $\vec{u}$ it will not contribute to the measured voltage signal, and the contribution will be maximum in absolute value if the two vectors are parallel. The contribution of a given local electromotive force density will be proportional to the magnitude of the local lead vector $\vec{u}(\vec{r})$. So, the stationary local lead

vector describes the sensitivity of the lead to a source located there. **The distribution of the lead vectors in the volume conductor is the lead field**, and this field gives the distribution of sensitivities of the system (the lead) formed by the volume conductor (biological tissues) and the electrodes.

It follows from **the reciprocity principle** [4] that the lead field $\vec{u}(\vec{r})$ is identical with the field of electric current density that is produced in the volume conductor when a unit current (called the reciprocal current) is fed to the lead from the outside. In our case one electrode will be active, concave, and located very close to the region of interest, and the other indifferent, with a much bigger surface, and far from this region.

In reference [1], assuming cylindrical symmetry in the electric potential field inside the volume conductor, approximated analytical formulae for the components of the lead vector field $\vec{u}(\vec{r})$ were obtained for any electrode's head size and shape, with the only restriction of the abovementioned imposed cylindrical symmetry and the assumed **homogeneity** and **isotropy** of the volume conductor. This was done starting from Whittaker's solution for Laplace's equation [6], using a multipolar expansion [7] of the electric potential along the axis of symmetry of the field.

It was shown that for concave electrodes of a suitably selected shape there is a **critical region**, of maximum sensitivity for sensing purposes, **located at a certain distance from the surface of the electrode**, where the density of lead field lines is higher than in any other region (including regions located nearer to electrode's concavity) and the lines are relatively parallel (Fig. 1).

Also, a generalization of formula (1) was derived for the measured potential difference between a proximal concave electrode and a distal indifferent one, due to tissues' electrical activity [1]. This formula, valid for **steady alternating currents** of a given (but arbitrary) frequency, may be applied even if the volume conductor is heterogeneous and anisotropic.

This second paper aims to:

(a) Review, from the standpoint of the lead field and the corresponding sensing sensitivities, some experimental results obtained in an electrolytic tank with metal electrodes of suitably enlarged sizes and made of a material showing strong polarization of the metal-electrolyte interface. Compare the results of the measurements with the mathematical model for concave electrodes immersed in homogeneous and isotropic volume conductors developed in [1].

(b) Derive for the time domain a generalized formula that gives the measured potential difference between a **polarizing** proximal concave electrode and a distal indifferent one, due to tissues' electrical activity, for transient's currents and voltages.

(c) Extend the design guidelines of concave electrode's heads (for attaining critical regions of suitable locations and sizes), briefly suggested in [1], to embrace the selective sensing of bioelectric signals generated in electromotive sources imbedded in heterogeneous and anisotropic tissues.

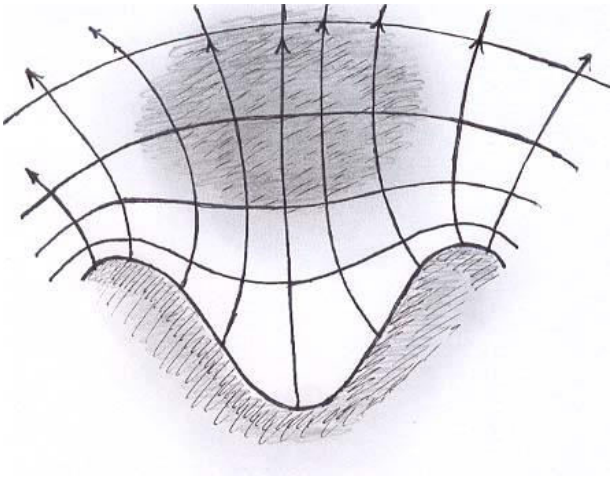

Fig.1: Pictorial representation, taken from [1], of a meridian cross section of a concave electrode, with a sketch of the lead field lines and of some surfaces of constant potential. The cross section of the critical region appears (in gray) as fuzzy elliptical.

Measurements of the lead field for concave electrodes

The surfaces of constant potential surrounding each type of a set of seven models of electrode heads of the same size but different shapes were measured in an electrolytic tank of 100 cm diameter and 80 cm height, with an electrically isolating internal surface (painted) [8],[9].

The indifferent electrode was made with a symmetric band of an aluminium foil stick to the inner side of the vertical wall of the tank.

The electrode heads (a hemispherical one, a planar one, and five different shapes of concave ones) were lathe machined on the top face of aluminium cylinders of 3 cm diameter and 3 cm height.

Each cylinder was mounted on an isolating (plastic) cylindrical support of 5 cm diameter and 5 cm height and located in the centre of the isolated bottom face of the tank.

The top face and the upper part of the curved vertical face of each cylinder were in electrical contact with the electrolyte, and the rest of the curved face was electrically isolated.

An Ag/AgCl measuring electrode was mounted in a vertical slender pipette, filled with a suitable electrolytic solution. Then the measured voltage may be assigned to the point where the tip of the pipette is located.

A controlled voltage source (dc and ac) was used to produce the fields in the electrolytic solution filling the tank. The measurements were made using a digital multimeter of very high input impedance. Also, an oscilloscope was used to register transients during sensing experiments with short current pulses. Figure 2 shows a sketch of the experimental arrangement.

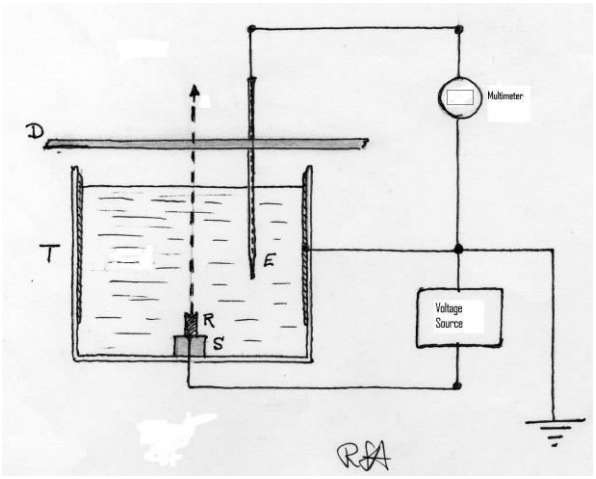

Fig. 2: Draft of the experimental arrangement. R, electrode; S, support; E, pipette with Ag/AgCl electrode; D, mechanical dispositive to locate the pipette; T, tank wall with the inner surface isolated and with the indifferent electrode stick to it.

In this paper we consider the measured lines of constant potential, in a plane through the axis of symmetry, for only two electrodes immersed in the electrolytic volume conductor of the tank: one representative of the concave electrodes (named **clothoidal** according to [3]), the other flat.

The measurements of the lines of equal potential were done with d.c. and once a steady state was established in the system. See figures 3 and 4:

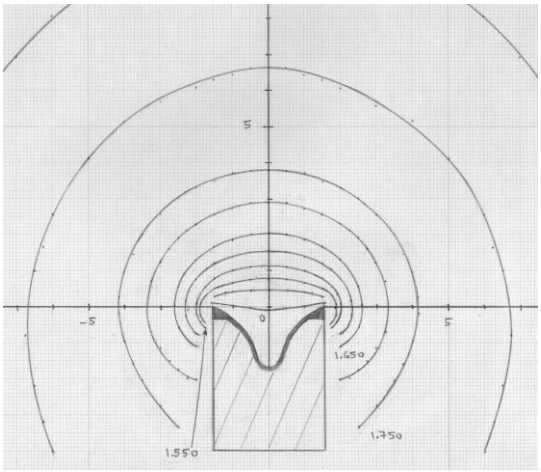

Fig.3: Distribution of lines of constant electric potential for a concave electrode in steady state. Difference of potential between adjacent lines: **0.05 V**

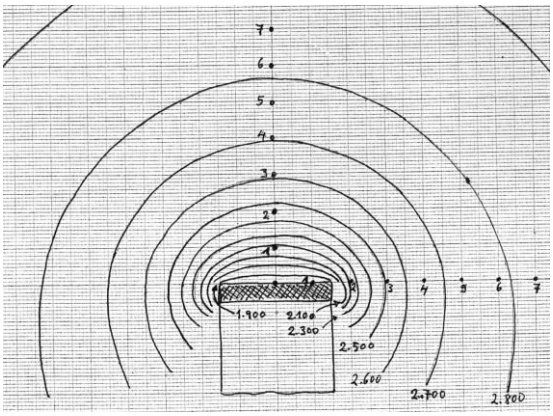

Fig.4: Distribution of lines of constant electric potential for a flat electrode in steady state. Difference of potential between adjacent lines: **0.10 V**

The corresponding orthogonal lines, giving a graphical representation of the lead field and its sensing sensitivities, could be approximately constructed from the lines of constant potential applying the classical drawing recipes of the old engineering field theory.

Instead of doing that, we use a mathematical model to connect the experimental results with the theoretical approach developed in [1].

Let us remind the formula for the potential near the axis of symmetry (where the critical region of highest sensing sensitivity of the concave electrodes is located:

$$V(\rho,z)=Z_0(z)+\rho^2 Z_2(z)+\rho^4 Z_4(z)+R(\rho,z) \tag{2}$$

Here ρ is the distance between the considered point and the axis of symmetry, and z is the coordinate on the axis.

With $V(0,z)=f(z)$:

$$Z_0(z)=f(z),\quad Z_2(z)=-\frac{1}{4}\frac{d^2 f(z)}{dz^2},$$

$$Z_4(z)=\frac{1}{64}\frac{d^4 f(z)}{dz^4}$$

The following expansion for the potential $V(0,z)$ should be enough for our purposes:

$$f(z)\approx\frac{I}{4\pi G}\left[\frac{1}{z}+\frac{\beta_2}{z^3}+\frac{\beta_3}{z^4}+c\right] \tag{3}$$

The remainder verifies: $R(\rho,z)=0(\rho^6)$

In the present case I is the global electric current injected by the voltage source in the steady state, and G is the electric conductivity of the electrolyte in the tank. The origin $z=0$ was suitably chosen at the electric centre of the distribution of field sources, so that the monopole coefficient $\beta_1=0$. In practice we only know that this centre must be on the axis of symmetry. So, let us choose the origin of coordinates in the point of intersection of the z axis with the upper face of the cylinder of the electrode, and measure distances d uppwards along the axis from this known point. Then

we put $z = r_0 + d$, being r_0 a new parameter, the so called "**electric radius**" of the electrode. For a perfectly spherical (and non-polarizable) electrode the geometric radius and the electric radius are equal.

After the mono-polar term, with $\beta_0 = 1$, we involve only the **quadrupole** and the **octupole** terms.

The multi-polar coefficients β_2 and β_3, as well as the electric radius r_0, must be determined from the experimental results.

The parameter c did not appear in the multipole expansion of the potential given in [1]. This expansion is valid when the volume conductor, besides being homogeneous and isotropic, may be considered infinite. The additional parameter must be introduced to take into account that now the volume conductor cannot be considered as unbounded. In general, the smaller the geometric dimensions of the electrolytic tank for a given electrode, the greater will be the number of additional parameters and additive terms necessary to quantify boundary effects on the spatial distribution of the electric potential.

In our case a single additive parameter is enough because: the geometric dimensions of the aluminium cylinders (radius 1.5 cm) are an order of magnitude less than the smallest dimension of the volume conductor (tank radius 50 cm, tank height 80 cm); the upper face of the electrode is located 8 cm from the isolated bottom of the tank; the indifferent electrode covers a significant part of the inside of the vertical wall leaving a relatively small isolating band in the lower part of the wall, band that begins slightly below the level of the electrode head (Fig. 2); and, finally, the electric potential measurements were taken mainly near the electrode head. A thorough discussion of boundary effects on the distribution of the potential in the electrolytic tank may be found [9].

Let us consider N values of the potential measured on the axis:

$$V(0, r_o + d_n) = V_n, n = 1,2,...,N$$

Then, a set of values of r_0, β_2, β_3 and c may be obtained minimizing the nonlinear expression

$$\chi^2(r_0, \beta_2, \beta_3, c) = \sum_{n=0}^{n=N} (f(r_0 + d_n, \beta_2, \beta_3, c) - V_n)^2 \quad (4a)$$

$$f(r_0 + d_n, \beta_2, \beta_3, c) \approx \frac{I}{4\pi G}\left[\frac{1}{r_0 + d_n} + \frac{\beta_2}{(r_0 + d_n)^3} + \frac{\beta_3}{(r_0 + d_n)^4} + c\right] \quad (4b)$$

This was done both for the concave and the flat electrode using the powerful Levenberg-Marquardt algorithm [10].

The following results were obtained from 15 measurements of the potential on the axis of symmetry for each electrode:

Clothoidal electrode:

$r_0 \approx 1.00$ cm, $\beta_2 \approx -0.53$ cm^2 $\beta_3 \approx 0.01$ cm^3, $c \approx 1.00$ cm^{-1}

Flat electrode:

$r_0 \approx 1.05$ cm, $\beta_2 \approx -0.40$ cm^2 $\beta_3 \approx 0.00$ cm^3, $c \approx 1.66$ cm^{-1}

In both cases the final Chi-squared values were of the order of 10^{-4}. The adjustment is very good. In fact, leaving aside, for obvious reasons, the hemispherical electrode, it was also very good for the other four types of concave electrodes of different shapes.

Three remarks are indicated to help to interpret the experimental results and the estimation of parameters presented above:

(a)The conductive surface in contact with the electrolytic solution (real exposed area) was approximately the same for the seven types of electrodes studied with the electrolytic tank.

(b) No difference was found between the surfaces of constant potential measured with a sustained a.c., 60 Hz, relative to those measured with d.c. in the steady state, although the measured points were not very near to the electrode surface.

(c) The polarization and other effects of the indifferent electrode can be neglected in this case.

Now, let us turn to the problem of determine the field of local sensitivities from the experimental results in the electrolytic tank. As was shown in [1], the local lead vector (sensitivity) $\vec{u}(\vec{r})$ may be calculated from its scalar components, axial $u_z = -\frac{\partial V}{\partial z}$ and radial $u_\rho = -\frac{\partial V}{\partial \rho}$ for a unit global current $I = 1$, using the first multi-polar coefficients β_2 and β_3 as the only parameters.

$$u_z \approx -\left[\frac{df(z)}{dz} - \frac{\rho^2}{4}\frac{d^3 f(z)}{dz^3} + \frac{\rho^4}{64}\frac{d^5 f(z)}{dz^5}\right] \quad (5a)$$

$$u_\rho \approx -\left[-\frac{\rho}{2}\frac{d^2 f(z)}{dz^2} + \frac{3\rho^3}{64}\frac{d^4 f(z)}{dz^4}\right] \quad (5b)$$

This presupposes that the location of the electric centre is known, which in practice, **is not the case**. However, using formula (3) with $z = r_0 + d$, we introduce a new unknown parameter (the electric radius) and the known distance (measurable) from the electrode head.

The parameter c, necessary to achieve a good adjustment between formula (3) and the measured values of the potential along the z axis, disappears from the formulae (5) because the components of the lead field are functions of the first and higher derivatives of (3).

The lead voltage: a formula in the time domain for sensing transient signals with polarisable electrodes.

Formula (1), reminded in the introduction, can be obtained under the following assumptions:

(a) The module of the input impedance of the measurement chain is, for all the frequencies involved in the biological electromotive sources, at least an order of magnitude greater than the module of the in-series combination of the impedance of the electrode's electrochemical double layer with the impedance of biological tissues.

(b) The effect, on the lead field, of the transients and non-uniformities in the polarization of the double layer located at the interface between the surface of the electrode head and the electrolytic volume conductor, may be neglected.

Note that when a direct current is established in an electrode-electrolytic system, (as is the case of the electrodes in the electrolytic tank studied in the precedent section), once the polarization of the double layer reaches a steady state, the lead vector field in each point of the volume conductor remains constant.

If the conductive medium is homogeneous and isotropic, the electric potential field may still be described by formulae (2) and (3) (with $z = r_0 + d$).

The steady and non-uniform polarization of the double layer appears implicit in the values of the parameters r_0 , β_2 , and β_3 .

In principle, if these parameters are given as suitable functions of time, the effect of transients and non-uniformities in the polarization of the double layer, on the axial u_z and radial u_ρ components of the lead field, could be described.

The non-uniform polarization of the double layer in non-spherical electrodes is related with the non-uniform distribution of the electric current density in the surface of the electrode, due to differences in the mean curvatures between points on the surface.

This non-uniform distribution is suggested in Figure 5 for a convex and non-polarisable electrode.

There, a continuous variation of the mean curvature is suggested in a cross section of the electrode. The point O represents the electric centre of the electrode.

The points S, P and Q are located on the same lead field line.

The dotted line between points O and S is a virtual prolongation of the lead field line.

It is possible to derive an analytical formula relating the magnitude of the lead field at each point of a field line with the curvatures of the congruence of orthogonal surfaces crossed by the line, by a suitable reinterpretation of results developed in [11].

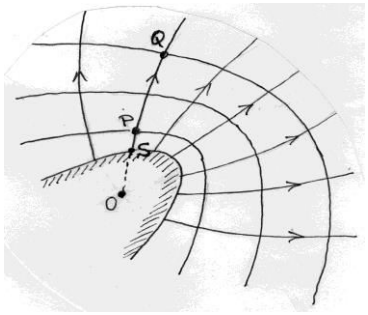

Fig. 5: Sketch of the distribution of the lead field lines and the surfaces of constant potential near a convex electrode surface immersed in a homogeneous and isotropic volume conductor.

This non-uniform distribution is suggested in Figure 5 for a convex and non-polarisable electrode. There, a continuous variation of the mean curvature is suggested in a cross section of the electrode. The point O represents the electric centre of the electrode. The points S, P and Q are located on the same lead field line. The dotted line between points O and S is a virtual prolongation of the lead field line. It is possible to derive an analytical formula relating the magnitude of the lead field at each point of a field line with the curvatures of the congruence of orthogonal surfaces crossed by the line, by a suitable reinterpretation of results developed in [11].

When an electrode surface is in equilibrium with an electrolytic solution, a steady and uniform potential difference appears between the two phases. If a direct current is injected through a highly polarizable flat electrode with a sharp edge, the potential drop in the double layer is modified: the dynamic perturbation is greater where the curvature is greater. At the fist moment after the current is applied, the perturbation is everywhere negligible, and the lead field (assumed quasi-static) corresponds to a truly flat electrode uniformly polarized. But as time goes on, a distribution of different potential drops in different places on the surface of the electrode begins to develop, and the corresponding lead field changes as it were produced by a family of non-polarizable virtual electrodes that change progressively their shapes, until arriving to a steady state. Each non polarizable virtual electrode may be characterized by its electric radius and its multipolar coefficients. The whole process can be described with a suitable set of time dependent parameters. Figure 6 suggests what happens once the steady state is arrived:

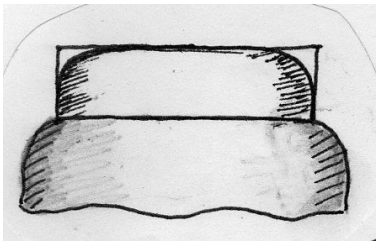

Fig. 6: Flat electrode strongly polarized in steady state, together with the equivalent virtual electrode in steady state.

The inner surface of the virtual electrode is practically coincident with the surface of the flat electrode in points where the curvature of this last one is zero (flat

upper face far from the edge) or relatively small (vertical face far from the edge). On the edge and near it, the virtual electrode is rounded and appears as smaller relative to the real flat one.

When the volume conductor is heterogeneous and anisotropic, the approach through the electric radius and the multipole coefficients doesn't apply. In [1] the generalization of formula (1) for the measured voltage signal in the time domain was done **in the frequency domain**.

For steady alternating current signals of frequency ω, finite input impedances of the chains of measurement $Z_{ext}(\omega)$ and non homogeneous and non isotropic volume conductors, taking into account the combined impedance $Z_T(\omega)$ of biological tissues and that produced by the polarization of the interface between the electrode and the tissues, the following formula was derived:

$$V_L(\omega) = \frac{1}{(1+\frac{Z_T(\omega)}{Z_{ext}(\omega)})}\left(\int_B \vec{u}(\omega,\vec{r})\cdot\vec{E}_S(\omega,\vec{r})\,d\nu\right) \tag{6}$$

The component $V_L(\omega)$ of the voltage sensed by the lead that corresponds to the angular frequency ω, is expressed as a functional of the distribution of vector electromotive forces, $\vec{E}_s(\omega,\vec{r})$, in the tissue's volume conductor, and the lead's vector field $\vec{u}(\omega,\vec{r})$ produced in the volume conductor by an alternating unit current injected from outside through the sensing electrodes and in steady state of oscillation. As mentioned above, the lead field may depend on the frequency due to the different degrees of polarization of the points on the surface of a concave electrode if the mean curvatures differ between these points.

Formula (6) is useful mainly when the spectral content of the signals doesn't change significantly with time.

But in biomedical engineering there are many circumstances in which the spectral content of relevant signals changes significantly during the interval of measurement, and a mixed time-frequency description may be necessary [12].

So, to allow the application of the powerful modern tools of signal analysis, a derivation in the time domain is advisable.

Let us begin with the general relation, equivalent to Equation (14) of [1], but written in the time domain:

$$\begin{aligned}&(\varphi_2(t)-\varphi_1(t))I'(t) = \\ &-V_L(t)I(t)+\int_B \vec{j}(t,\vec{r})\cdot\vec{E}_S(t,\vec{r})\,d\nu\end{aligned} \tag{7}$$

Equation (7) can be derived from a version of the reciprocity theorem formulated for the so-called quasistatic approximation to the electromagnetic field.

To simplify the derivation, let us suppose that the ohmic component of the external circuit impedance, R_{ext}, is dominant. Then, the voltage signal (lead voltage between the electrodes) $V_L(t)$ and the current I' produced by the bioelectric electromotive forces are related by:

$$V_L(t) \approx R_{ex}\, I'(t) \tag{8}$$

The injected current I produced by an external applied potential difference between the electrodes $\varphi_2 - \varphi_1$, is assumed constant: the applied potential difference must be adjusted to comply with this restriction while the electrode´s electrochemical double layer polarizes.

Then, if R_T is the resistance of the volume conductor of the tissues and $\int_0^t K(u)\,du$ is the voltage drop in the double layer:

$$\varphi_2 - \varphi_1 = \left(R_T + \int_0^t K(u)\,du\right) I \tag{9}$$

(In [13] may be found a short presentation of this kind of mathematical model of the electric behavior of polarizable electrodes in volume conductors).

From (7), (8) and (9), if R_{ext} is at least an order of magnitude greater than $R_T + \int_0^t K(u)\,du$, follows the approximate formula in the time domain, that may be applied to arbitrary, non-homogeneous and anisotropic, albeit ohmic volume conductors:

$$V_L(t) \approx \int_B \vec{u}(t,\vec{r})\cdot E_S(t,\vec{r})\,dv \tag{10}$$

In this formula (a direct extension of Equation (1)) the effect of the non-uniform and transient polarization of the double layer of the active electrode on the lead field $\vec{u}(t,\vec{r}) = \frac{1}{I}\vec{j}(t,\vec{r})$ is included introducing an explicit time dependence that must be calculated from the electric, geometric, and electrochemical properties of the system.

But for many tissues, and in the case of myocardium in particular, the volume conductor is anisotropic and heterogeneous, and certainly bounded, so the study of the relation between the size and shape of the electrode's head and the generated lead field $\vec{u}(t,\vec{r})$, including the location and geometric dimensions of the critical region for sensing bioelectric signals, should be extended to embrace this more general case.

Introduction of an auxiliary virtual space (alibi)

For common types of heterogeneity and anisotropy, like the ones found in ventricular myocardium, a change of spatial variables from Euclidean to curvilinear coordinates may be found, allowing the reduction of several complex three- dimensional propagation problems of action potentials to propagation in the homogeneous and isotropic case, if an auxiliary "**virtual space**" with a smooth one to one correspondence with physical space, is introduced [14].

It is possible to apply this idea of an auxiliary space (alibi), to the description of the sensing sensitivity field (lead field) of an active electrode in a volume conductor.

In the auxiliary space, Laplace's equation for the potential and all the previous developments are valid, including the approximate analytical formulae relating the geometrical dimensions of the critical region with the distribution of electric potential along the axis of symmetry of the concave active electrode given in [1]. Going back to the original coordinates, the results are interpreted in physical space and the modifications that the lead field and the sensing sensitivities suffer due to the anisotropy and heterogeneity of the tissues are assessed.

Let us briefly sketch the procedure by a typical example: the myocardium. (All the necessary background information that is needed from now on may be found in [15]).

We assume that a small sensing electrode is localized in the ventricular cavity, touching the endocardium.

The endocardial surface may be represented, approximately enough, as a plane.

The myocardial fibres run almost parallel in layers, but the direction of the fibres in each layer varies smoothly from the endocardium to the epycardium.

We introduce first a trihedral T_0 of unit vectors, $\vec{i}_0, \vec{j}_0, \vec{k}_0$ with the origin and the unit vectors $\vec{i}_0, \vec{j}_0$ fixed in the endocardial plane, and $\vec{k}_0$ orthogonal to this plane and pointing towards the epycardium.

Now, taking as new origin each point of coordinate z of the line defined by $\vec{k}_0$ and the origin of T_0, we introduce a new orthogonal trihedral T_z of unit vectors $\vec{e}_1 = \vec{e}_f, \vec{e}_2, \vec{e}_3 = \vec{k}_0$, where $\vec{e}_f$ gives the direction of the fibres in the layer located at a depth z from the endocardium.

Then any point in the myocardium may be given by the coordinate z and its three coordinates x_1, x_2, x_3 relative to T_z.

The following connection exist between the coordinates x, y relative to T_0 and x_1, x_2 relative to T_z:

$$x_1 = x\sin\left[\alpha\ z\ \right] + y\cos\left[\alpha\ z\ \right] \qquad (11a)$$

$$x_2 = -x\cos\left[\alpha\ z\ \right] + y\sin\left[\alpha\ z\ \right] \qquad (11b)$$

Here $\alpha(z)$ is the angle between the direction of the fibres in the layer, $\vec{e}_f$ and the unit vector $\vec{j}_0$.

If $\hat{G}$ is the conductivity tensor and V the electric potential, then:

$$\nabla\cdot(\hat{G}\cdot\nabla V) = 0 \qquad (12)$$

Now, the conductivity tensor of the volume conductor is diagonal relative to T_z in the corresponding layer of myocardial fibres.

With enough approximation, its diagonal components G_{11}, G_{22}, G_{33} are functions of only one coordinate:

$$G_{11}(x_2),\ G_{22}(x_2),\ G_{33}(x_3)$$

As consequence, if $V(x_1, x_2, x_3)$ is the representation of the electric potential in local coordinates, equation (12) may be written thus:

$$\sum_{n=1}^{3}\frac{\partial}{\partial x_n}[G_n(x_n)\frac{\partial}{\partial x_n}V] = 0 \qquad (13)$$

Nevertheless, we are still in physical space, naming the same points in another form (alias, using other coordinates).

Now, let us introduce a virtual space (alibi) of coordinates ξ_1, ξ_2, ξ_3, filled by a homogeneous and isotropic volume conductor of arbitrary (scalar) conductivity G_0.

The connection between corresponding points of each space is given by:

$$\xi_k \approx \int_0^{x_k}\sqrt{\frac{G_0}{G_{kk}(s)}}\,ds \qquad k = 1,2,3 \qquad (14)$$

The connection between the local representation of the potential in physical space $V(x_1, x_2, x_3)$ and the potential in the corresponding point of virtual space virtual space $\psi(\xi_1, \xi_2, \xi_3)$ is defined by:

$$\psi(\xi_1, \xi_2, \xi_3) = V(x_1(\xi_1), x_2(\xi_2), x_3(\xi_3)) \qquad (15)$$

Furthermore, we introduce the functions:

$$g_{kk}(\xi_k) = G_{kk}(x_k(\xi_k)) \qquad k = 1,2,3 \qquad (16)$$

The, from (14), (15) and (16), the left-hand member of (13) may be shown to be equal to:

$$G_0\left[\sum_{k=1}^{3}\frac{\partial^2\psi}{\partial\xi_k^2} + \frac{1}{2}\sum_{k=1}^{3}(\frac{1}{g_{kk}}\frac{dg_{kk}}{d\xi_k})(\frac{\partial\psi}{\partial\xi_k})\right] \qquad (17)$$

So (13) is equivalent to:

$$\sum_{k=1}^{3}\frac{\partial^2\psi}{\partial\xi_k^2}(1 + \frac{1}{2}\frac{L_{\psi,kk}}{L_{g,kk}}) = 0 \qquad (18)$$

Here: $L_{\psi,kk} \approx \dfrac{(\dfrac{\partial \psi}{\partial \xi_k})}{(\dfrac{\partial^2 \psi}{\partial \xi_k^2})}$ (19a) $L_{g,kk} \approx \dfrac{g_{kk}}{\dfrac{dg_{kk}}{d\xi_k}}$ (19b)

If the spatial scales of the components of the gradient of the potential (the components of the electrical field) in virtual space $L_{\psi,kk}$ are (as a rule) at least an order of magnitude less than the spatial scales of the components of the conductivity tensor in virtual space $L_{g,kk}$, then the potential in the auxiliary space $\psi(\xi_1, \xi_2, \xi_3)$ will verify, approximately Laplace's equation:

$$\sum_{k=1}^{3} \frac{\partial^2 \psi}{\partial \xi_k^2} \approx 0 \qquad (20)$$

The approximation will be better the smaller are the quotients of the spatial scales $L_{\psi,kk}$ and $L_{g,kk}$.

Conclusions

(a) An experimental procedure for a parametric characterization of the lead field of sensing electrodes (concaves or not) from experimental data was described.

Giving the good adjustment obtained by the application of Levenberg-Marquardt algorithm, and introducing the experimental values of r_0, β_2, and β_3, then the components of the lead field of a polarizable electrode, in steady state and immersed in an electrolytic solution, could be predicted using formulae (5), at least near the axis of symmetry where the critical region of higher sensing sensitivity of concave electrodes is located. This kind of experiment in electrolytic tanks, with active electrodes of scaled sizes, and with suitable surface microstructures, allows an easy determination of the lead fields and the corresponding sensing sensitivities when the double layer is polarisable and polarizes non-uniformly, like in concave electrodes.

(b) For unbounded, isotropic, and homogeneous volume conductors, the time dependence of the lead field of a polarizable active may be traced back to an explicit time dependence electrode of the coefficients of the multipolar expansion of the electric potential.

The multipolar coefficients β_2 and β_3 can then be related, at its turn, with the size and shape of the sensing electrode's head.

Then, formula (10) can be used to relate the voltage signal in each lead with the distribution of biological electromotive forces that produce it, for measurement chains of input impedance at least an order of magnitude greater than the impedance of the lead system itself.

An extension of formula (10) to the case in which this last assumption doesn't apply would be of interest.

(c) The design problem of determining the geometric parameters of an electrode's head such that it produces a critical sensing region for bioelectric signals, with suitable shape and size, as was posed and solved in [1] for homogeneous and isotropic volume conductors, can be extended to heterogeneous and anisotropic volume conductors introducing a virtual space that allows a reduction of the problem to the formerly solved one. After that the results can be translated to the heterogeneous and anisotropic case in physical space.

(d) As the electric conductivity of the electrode's material is at least several orders of magnitude greater than the conductivity of the tissues and the body fluids, the surface of the electrode may be safely assumed to be a surface of constant value of the electric potential field V produced when the reciprocal current is injected to the lead from outside.

In principle any surface V =constant in the virtual space could be a candidate to a surface of a suitable electrode, and for each one of this, we have a corresponding surface in physical space.

However, this cannot be exactly this way if the surface of equal potential is unbounded in physical space.

But if our interest is focussed into the abovementioned critical region located near the axis of symmetry, it is possible to construct a suitable approximation to the shape and size of the electrode to produce the desired lead field and thus the desired distribution of local sensitivities within established tolerance bounds, as shown in [1].

(e) Now, it seems that enough groundwork has been done to enable an efficient application of numerical codes for elliptic partial differential equations to design problems posed by the sensing of bioelectric signals by concave electrodes.

Nevertheless, the digital simulation of the non-uniform polarization process coupled with the field equations poses several problems.

This, as well as specific examples of design of concave electrodes for sensing bioelectric signal will be the purpose of the last paper in this series.

References

[1] R. Suárez-Ántola "*Sensing bioelectric fields with concave electrodes. I Lead fields and sensitivity*", Proceedings of the 5th Ibero-American Congress on Sensors), Montevideo, Uruguay, 27-29 September 2006. (In CD-ROM).

[2] A. Amiel, J. Besson and G. Lehmann: "*The convergent field tip: A clinical comparison with regular leads*", in A.Aubert and H.Hector (Eds) "Pacemakers leads", Amsterdam: Elsevier, 1985.

[3] O. Fiandra and R. Suárez-Antola: "*Electrode for electric stimulation of living tissues*", *UY*- Patent *12.817*, Montevideo, 1987.

[4] J. Malmivuo, "*Biomagnetism*", Chapter 27 in *"Biomedical Engineering Fundamentals",* J.Bronzino (Ed.), *"*The Biomedical Engineering Handbook*",* 3ª Ed, Boca-Raton: CRC, Taylor & Francis Group, 2006.

[5] R. Arzbaecher and D. Brody, "*The lead field: vector and tensor properties*", Chapter 7 in C.Nelson and D.Geselowitz (Eds.), "The theoretical basis of electrocardiology", Clarendon Press, Oxford, 1976.

[6] E. Copson, "Partial Differential Equations", Chapter 11, Cambridge University Press, Cambridge, 1975.

[7] J. D. Jackson, "Classical Electrodynamics", Wiley, N.Y., pp 136-143, 1975.

[8] R. Suárez-Ántola, J. Griego and O. Fiandra: "*Concave electrodes I: Experimental foundations*", World Congress in Medical Physics and Biomedical Engineering, Rio de Janeiro, Brazil, 21-26 August 1994; abstract published in Physics in Medicine and Biology, vol.39a, p 413, 1994.

[9] R. Suárez-Antola: "*Biophysical foundations for the study of electric excitation and action potential propagation in myocardium*", M.Sc. Thesis (in Spanish), PEDECIBA, UDELAR, Montevideo, Uruguay, pp 92-112, 1991. (Available in electronic form from biblioteca@dinamige.miem.gub.uy)

[10] W. Press, S. Teukolsky, W. Vetterling, and B.Flannery: "Numerical Recipes in Fortran", 2nd Edition, Cambridge University Press, Cambridge, UK, Chapter 15, pp678-683, 1992.

[11] R. Suárez-Ántola, "*Chronic cardiac pacing: a bio-mathematical approach*" in O.Fiandra (Ed.), "Cardiac Pacemakers", CCC, Montevideo, Uruguay, pp145-148, 1985.
(In Spanish, although a translation to English of Chapter 8 was made under the request of Professor S.Furman M.D.).

[12] A. Ritter, S. Reisman and B. Michniak: "Biomedical Engineering Principles", CRC, Taylor & Francis Group, N.Y., USA, pp293-303, 2005.

[13] R. Suárez-Ántola; *"The time constants for cathodic make stimulation of electrical syncytia: an application to cardiac pacing",* Proceedings of the 28th Annual International Conference IEEE-Engineering in Medicine and Biology Society, New York, USA, pp 4031-4034, 2006.

[14] R. Suárez-Ántola: "*Thresholds: Contributions to the study of excitation and propagation of the electric activity of biological tissues stimulated by external electrodes*", D.Sc. Thesis, PEDECIBA, UDELAR, Montevideo, Uruguay, Chapter VII, pp41-48, 1994.

[15] D. Zipes and J. Jalife (Eds) "Cardiac Electrophysiology: from cell to bedside", 2nd Edition, W.Saunders, Philadelphia, USA, Part IV, Chapter 25 and Part V, Chapter 30, 2004.